Hochschule für Angewandte Wissenschaften Hamburg

Hamburg University of Applied Sciences

Project Thesis

Department Fahrzeugtechnik und Flugzeugbau

Flight Dynamic Investigations of a Blended Wing Body Aircraft

Author: Christoph Neubacher

Examiner: Prof. Dr.-Ing. Dieter Scholz, MSME

Date of Submission: 1.10.2008

Abstract

This thesis deals with stability investigations and a motion simulation of a non conventional aircraft configuration. The investigated aircraft of this thesis is called AC 20.30 and is a Blended Wing Body model aircraft, which was designed by a research group of students of the University of Applied Science Hamburg. The stability investigations of the AC 20.30 should show, if the aircraft is statically and dynamically stable for the longitudinal and lateral motion. The aircraft stability can be computed with the help of the stability derivatives computed with the aerodynamic coefficients measured in the Wind tunnel Dresden. As a result of the stability investigation, the AC 20.30 shows for two characteristics motion modes of the longitudinal motion, the Phugoid mode and the Short Period mode, dynamically stable behaviour. The stability investigation for the lateral motion results in dynamically stable flight characteristics for the Roll and Dutch Roll mode, while the AC 20.30 is dynamically unstable for the Spiral mode. Additional to the stability investigation the AC 20.30 is investigated for its flight characteristic and is classified into flight levels. The AC 20.30 shows for the longitudinal motion level 1 flight characteristics, while the flight characteristics for the lateral motion are between level 1 and 2. The motion simulation of the AC 20.30 takes place in the Matlab Simulink environment. It should simulate, how the AC 20.30 acts in its different motion directions, if the control surfaces are deflected or if suddenly appearing gusts affect the aircraft. The simulation should also show, whether or not the aircraft is able to damp out the mentioned disturbances in the motion directions.

DEPARTMENT FAHRZEUGTECHNIK UND FLUGZEUBAU

Untersuchungen zur Flugdynamik des Blended Wing Body

Aufgabenstellung für ein *Projekt 2*

Hintergrund

Am Studiendepartment wurde ein Flugmodell in einer Blended Wing Body (BWB) Konfiguration gebaut und im Windkanal in Dresden vermessen.

Aufgabe

Bei Windkanalversuchen mit dem Flugmodell wurden in verschiedenen Messreihen aufgezeichnet: Auftrieb, Nickmoment, Widerstand, Seitenkraft, Giermoment, Rollmoment, Anstellwinkel, Schiebewinkel und Windkanalstaudruck. Aus den gewonnenen Daten sollen Beiwerte der Flugdynamik gewonnen werden, um damit anschließend Simulationen der Längsbewegung (und evtl. auch der Seitenbewegung) des BWB durchführen zu können.

Die Rechnungen/Simulationen sollen mit MATLAB/Simulink durchgeführt werden.

Die Ergebnisse sollen in einem Bericht dokumentiert werden. Bei der Erstellung des Berichtes sind die entsprechenden DIN-Normen zu beachten.

Contents

List of Figures

List of Tables

Nomenclature

Latin Letters

A	State coefficient matrix
a_y	Side slip acceleration
a_z	Acceleration in z-direction
b	Wing span
B	Driving matrix
C	Output matrix
$\bar{c}$	Mean aerodynamic chord line
C_D	Drag coefficient
C_{D_α}	Drag curve slope
C_{D_u}	Change in the drag coefficient caused by the change in the velocity
C_{D_δ}	Change in the drag coefficient due deflection of the control surfaces
C_l	Rolling moment coefficient
C_L	Lift coefficient
C_{L_α}	Lift curve slope
C_{L_β}	Change in C_l due to a change in the side slip angle
C_{L_δ}	Change in the lift coefficient due flap or elevator deflection
C_{L_u}	Change in the lift coefficient caused by the change in the velocity
C_m	Pitching moment coefficient
C_{m_0}	Pitching moment coefficient of the wing
C_{m_α}	Slope of C_m - α plot
C_{m_δ}	Change in the pitching moment coefficient due deflection of control surfaces
C_n	Yawing moment coefficient
C_{n_β}	Change in C_n due to a change in the side slip angle
C_{n_δ}	Change in C_n due to the deflection of the control surfaces
C_y	Side force coefficient
C_{y_δ}	Change in C_y due to the deflection of the control surfaces
$\vec{d}$	Source of disturbance vector
D	Feed forward matrix
E	Associated matrix for the state equation
g	Acceleration due to gravity
i	Complex number
I	Identity matrix
I_x	Moment of inertia in roll direction
I_y	Moment of inertia in pitch direction
I_z	Moment of inertia in yaw direction
l, m, n	Dimensions of the matrix
L_β	Dihedral effect

L_p	Roll damping
L_r	Rolling moment due yaw rate
l_t	Length of the tail
M	Mach number
M_δ	Change in the pitching moment due to elevator or flaps deflection
M_y	Pitching moment
m	Mass of the aircraft
$\tilde{M}_\delta$	"Tilde" derivative of the control related derivative
M_u	Stability derivatives of the longitudinal motion in u-direction
M_w	Stability derivatives of the longitudinal motion in w-direction
M_g	Stability derivatives of the longitudinal motion in q-direction
M_θ	Stability derivatives of the longitudinal motion in θ-direction
$\tilde{M}_i$	"Tilde" stability derivatives of the longitudinal motion
$M_{\dot{w}}$	Damping stability derivative
n_α	Acceleration sensitivity
N_β	Directional stability
N_p	Yawing moment due roll rate
N_r	Yaw rate damping
$n_{z_{cg}}$	Load factor
p	Roll rate
q	Dynamic pressure
r	Yawing rate
s	Variable for the second order equation
S	Wing area
T	Wavelength
T_s	Time to double
T_{ξ_R}	Roll time constant
u	velocity
U_0	Air speed
$\vec{u}$	Control input variables
X	Axial force
x_{ac}	Position of the aerodynamic center
x_{cg}	Position of the center of gravity
X_δ	Stability derivative of the axial force X due to control surface deflection
X_u	Stability derivatives of the aerodynamic force X in u-direction
X_w	Stability derivatives of the aerodynamic force X in w-direction
$\vec{x}$	State vector
$\dot{\vec{x}}$	State variables
Y	Side force
$\vec{y}$	Output vector
Y_β	Side force due to a change in side slip angle

y_δ	Change in the side force due to control surface deflection
Y_p	Side force due to yaw rate
Z	Normal force
Z_δ	Change in the normal force caused by control surface deflection
Z_u	Stability derivatives of the normal force in u-direction
Z_w	Stability derivatives of the normal force in w-direction

Greek Letters

α	Angle of attack
γ	Flight path angle
κ	Specific heat ratio
λ	Eigenvalue
Λ	Aspect ratio
ν	Side slip velocity
ϕ	Angle of blank
ρ	Density
θ_0	Pitch attitude
σ	Real part value
ω	Frequency
ξ	Damping ratio
ψ	Heading angle

Subscripts

A	Aileron
ac	Aerodynamic center
cg	Center of gravity
d	damped
e	Elevator
n	naturally
p	Roll rate
ph	Phugoid mode
r	Yaw rate
R	Rudder
$RearEnd$	Flap pair located at the rear end
sm	Spiral mode
sp	Short period mode
$Wing$	Flap pair located at the wing

Abbreviations

AC	Aircraft
BWB	Blended wing body
CATIA	Computer aided three-dimensional interactive application
CAD	Computer aided design
CAP	Control anticipation parameter
CFD	Computational fluid dynamics
CG	Center of gravity
DLR	German Aerospace Center
FAA	Federal Aviation Administration
HAW	University of Applied Science
HTP	Horizontal tail plane
ODE	Ordinary differential equations
USA	United States of America
VTP	Vertical tail plane

1 Introduction

1.1 Motivation

The aircraft market is a fast growing but also competitive business. Therefore the aircraft building companies invest a lot of effort into the research for new aircraft configurations to be one step ahead of the other companies to accomplish the given constraints and requirements for the aircraft market of tomorrow. One of the results of these researches is the blended wing body aircraft (BWB). The BWB is a non conventional aircraft configuration. The characteristic of the BWB is that not only the wing produces lift as for the conventional aircraft common, the fuselage produces lift as well. This deals with the fact that the fuselage is designed like a lift producing airfoil for even small angles of attack.

Another advantage of this design is that the fuselage offers more room for payload compared to the conventional aircraft with a comparable span size. This makes the BWB an alternative to conventional aircraft for the market of tomorrow.

A major disadvantage of the BWB is the flight stability. At the moment this aircraft type is only used for military applications. To design the first BWB for civil use the HAW - Hamburg put a lot of effort in their BWB project. The HAW - Hamburg designed a model of a BWB for flight tests the AC 20.30. After the AC 20.30 passed its flight tests aerodynamic investigations in the wind tunnel Dresden were run. The goal of these investigations was to measure the different aerodynamic characteristic coefficient of the AC 20.30 for different angle of attacks, different side slip angle and rudder, flap, aileron, spoiler, elevator deflections. These aerodynamic coefficients of the test were provided and introduced by **Zingel 2006**. As mentioned in this thesis the wind tunnel results show some discrepancies because the used wind tunnel model was actually developed and designed for flight tests and not for wind tunnel tests.

With the help of these aerodynamic coefficients the stability of the BWB can be described. Therefore, the aerodynamic coefficients have to be computed in flight dynamic parameters to investigate the stability of the BWB for lateral and longitudinal motion.

After the flight dynamic parameters are computed, a simulation of the stability behaviour of the BWB for different flight maneuvers (e.g. flap, rudder, elevator, aileron deflection) is designed in Matlab Simulink environment to visualize the flight behaviour of the BWB.

1.2 Definitions

Adverse Yaw

The adverse yaw takes place if the ailerons are deflected for a spiraling maneuver. It is a yaw moment to the opposite maneuver direction and has to be neutralized by a rudder deflection.

Aircraft Control

The aircraft control directs the movements of an aircraft with particular control surfaces. In addition to the direction, the altitude and the aircraft velocity can be also directed.

Dihedral

Dihedral is the upward angle from the horizontal in a fixed wing aircraft and goes from the root to the tip. The purpose of positive dihedral angle of the wing is to produce stability in the longitudinal (roll) axis. The most civil transport aircraft are designed with a positive dihedral angle of the wing to avoid roll instability.

Eigenvalues

It is the factor of dilation for the eigenvectors.

Eigenvector

An eigenvector of a given linear transformation is a non zero vector and its direction does not change due the transformation. So the eigenvector experiences a dilation and the factor of the dilation is called eigenvalue.

Gust

A gust is an inconstant wind. It is characterized by the appearance rapid change in the force and/or the direction of the wind. The gust appears in a blast of varying strength with brief lulls.

Linear Interpolation

The linear Interpolation finds its use, if two known points are given by their coordinates (x_1, y_1) and (x_2, y_2). The linear interpolant is a straight line between these points. With the help of the linear interpolation for a given x value in the interval (x_1, x_2) the corresponding y value can be computed. The linear interpolation formula has following definition:

$$y = y_1 + (x - x_1) \cdot \left(\frac{y_2 - y_1}{x_2 - x_1} \right)$$

Matlab Simulink

Matlab Simulink is a tool for modeling, simulating and analyzing multi-domain dynamic systems. It is a graphical block tool and is often used for control engineer applications.

State Equation

The state equation is a physical equation describing the state of matter under a given set of physical conditions. It is a constitutive equation, which provides a mathematical relationship between two or more state functions.

Static Margin

The static margin is used to characterize the static stability and controllability of an aircraft.

Trimmed Condition

If the aircraft is put in a state of equilibrium e.g. by adjusting control inputs, then the aircraft is flying in trimmed condition.

Wavelength

Under physical aspects the wavelength is the distance between repeating units of a propagating wave of a given frequency. The wavelength is related to the frequency, because the wavelength is inversely proportional to frequency. The higher the value of the frequency is the smaller is the wavelength.

1.3 Objective of this Thesis

The objective of this thesis is to compute given aerodynamic coefficients of the AC 20.30 provided by Till Zingel into relevant flight dynamic parameters to perform flight dynamic stability investigations of the AC 20.30 for the lateral and longitudinal motion. Further it is to create a MATLAB Simulink model to simulate the lateral and longitudinal motion of the AC 20.30.

1.4 Literature Survey

The most literature of the flight dynamic is written in the English language, therefore most of the here mentioned literature is based on the English language.

The book "Automatic Flight Control Systems" written by **Mc CLean 1990** is the major literature source for the converting of the aerodynamic parameters into the flight dynamic parameters and for the computation of the dynamic stability behaviour of the investigated aircraft introduced in this thesis. Further the flight dynamic lecture at the HAW-Hamburg in the Department Flugzeugbau is based on this book.

The book "Flight Stability and Automatic Control" written by **Nelson 1998** is used in this thesis as a literature source for the definitions of the static and dynamic stability and for the definition of the flying qualities. The explanations of the different stabilities of an aircraft are easy to follow and there a good examples for the different stability behaviours of an aircraft are chosen. In addition to this the book gives a good overview of the required stability derivatives for the lateral and longitudinal motion.

To create the simulation in the Matlab Simulink environment the "Symbolic Math Toolbox" **Matlab User's Guide 2002** is used. It is helpful to guide through the complex world of Matlab Simulink. It shows the user with the help of examples the acquaintance with Simulink for building models to solve control engineering problems.

The additional literature of this thesis can be examined in the bibliography of this thesis.

1.5 Layout of this Thesis

The layout of should give a fast overview of the main chapters of this thesis

- The thesis is based on the converting the aerodynamic parameters into flight dynamic parameters and further on a calculation and simulation of the longitudinal and lateral motion of a blended wing body.

- The declaration of the used definitions should help the reader to avoid misunderstanding

- The literature survey should give an overview and should introduce the most important literature sources for this thesis to get further information and detail informations, which are not mentioned in this thesis.

- The main part of this thesis contains the explanations for the following subjects:

  Chapter 2: deals with the introduction to the control related components of an aircraft

  Chapter 3: introduces the blended wing body concept and the AC 20.30 project

  Chapter 4: gives an overview of the flight conditions and the reference axis system

  Chapter 5: defines the motion related parameters in the flight dynamics

  Chapter 6: describes the theory of the static and dynamic stability and how the stability of an aircraft can be computed with the help of the coefficient matrix A for the lateral and longitudinal motion.

  Chapter 7: deals with the stability investigation for the AC 20.30 with the help of the flight parameters and the methods introduced in Chapter 5 and 6

  Chapter 8: shows the required input data for the simulation of the longitudinal and lateral motion in the Matlab Simulink environment for the AC 20.30 and a description of the design process of this simulation.

  Chapter 9: shows future prospective for an upcoming investigation based on this thesis

  Chapter 10: is the conclusion of this thesis including a discussion of the results and of the Matlab Simulink simulation

2 Introduction to Control related Aircraft Components

2.1 Overview

These section should give a small over view of the most important control related aircraft components and their main functions and influences to the control of an aircraft. The introduced aircraft components in this chapter are:

- Ailerons
- Flaps
- Elevator
- Vertical Tail Plane

The location of these control related aircraft components can be seen in Figure 2.1:
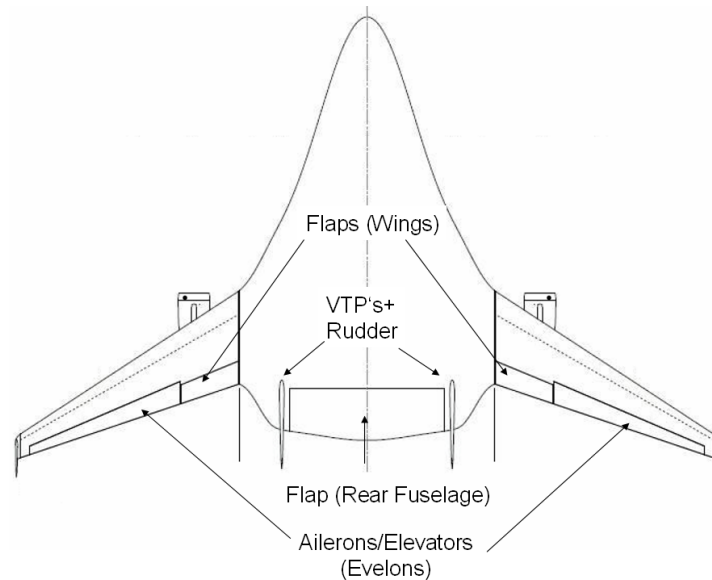
Figure 2.1: Location of the Control Surfaces

2.2 Ailerons

Ailerons are hinge control surfaces located outboard on the wing. The word aileron is French and the translation of it stands for "little wing".

Usually an aircraft has two ailerons which interacts with each other. The basic principle behind the ailerons is to modify the spanwise lift distribution, so that a moment is created about the longitudinal axis. To create this moment one Aileron has an upward deflection and decreases the lift of the wing, while the other aileron deflects downward and increases the lift on the other wing. This interacting of the ailerons leads to an imbalance around the longitudinal axis, the so called roll moment. During the Aileron operation an unwanted side effect of the Aileron appears the adverse yaw. It is a yawing moment in the opposite direction to the turn by the ailerons. Simplified means this that a roll moment caused by the Ailerons to the right produces a yawing moment to left. This has to deal with the fact that the rising wing tilts back its lift and produces an aft force component. The descending wing tilts the lift vector forward and that results in a forward force component. These forces on the opposite wing tips are the main reason for the adverse yaw. An additional source for the adverse yaw is the profile drag difference between the upwards deflected aileron and the downward deflected aileron.

An usual method to compensate the adverse yaw is the use of the rudder. The rudder has to be deflected in the opposing direction to the yaw direction caused by the adverse yaw. These deflection produces a side force on the vertical tail, which results in an opposing yaw moment to compensate the adverse yaw. Another method to compensate the adverse yaw is caused by differential ailerons. These ailerons have to be designed that the downward moving aileron deflects less than the upward moving aileron.

For the investigated aircraft of this thesis a special kind of ailerons have to be used as seen in Figure 2.1. A combination of aileron and elevator is used, which is referred as Elevon in the literature. It works as an elevator, when both flaps are deflected to the same direction (e.g. downward) and it works as an aileron when the flaps are deflected in different direction (e.g. left down - right up).

2.3 Elevators

The elevators are also known as stabilators in the literature. They are control surfaces usually located at the rear end of an aircraft. The objective of the elevators is to control the aircraft orientation by changing the pitch of the aircraft, which leads to a change of the angle of attack. An increase of the angle of attack will cause a greater lift to be produced by the airfoil of the wing, which decelerates the aircraft on the other hand, while a decrease of the angle of attack accelerates the aircraft. For conventional aircraft configuration the elevators are part of the horizontal tail plane (HTP). But the BWB

is a non conventional aircraft, which does not have a HTP, therefore the elevator has to be located at the wing as mentioned in Section 2.2.

2.4 Flaps

The flaps are part of the high lift devices system for modern transport aircraft. They are hinged surfaces on the trailing edge of the wings as seen in Figure 2.2.

Figure 2.2: Extended Flaps during Landing (**Airliners 2008**)

As flaps are extended the stalling speed of the aircraft is reduced. The extension of the flaps also increases the drag coefficient of the aircraft for any weight or airspeed. One reason for the higher drag coefficient is the result of the higher induced drag caused by the distorted planform of the wing due to the extended flaps. Another reason for the higher drag coefficient is the increase of the wetted area of the wing caused by the flaps extension. The increase of the wetted area results in an increase of the parasitic drag component of the total drag, hence it increases the drag coefficient.

Most aircraft extend their flaps partially during take off to decrease the required runway length. The partially extended flaps give the aircraft a slower stalling speed with a

small increase of the drag. The slower stalling speed allows the aircraft to take off in a shorter runway distance. The flaps are usually fully extended during landing to give the aircraft a slower stalling speed. This allows the aircraft to fly the approach with a slower velocity, but the wing still produces enough lift to keep the aircraft in trimmed condition during the approach flight. A pleasant side effect of the fully extended flaps is the higher drag coefficients, which decreases the aircraft velocity during the approach flight. A slower approach velocity of an aircraft means, that the aircraft requires a shorter runway distance.

2.5 Spoilers

The spoiler is also known in the literature as lift dumper. It is a device to reduce the lift of an aircraft. Spoilers are located on the top of wings and can be expended as seen in Figure 2.3.

Figure 2.3: Spoilers (**Airliners 2008**)

While they are extended, they create a controlled stall over the wing sections, which are located behind the spoilers. If the spoiler are extended symmetrically during cruise flight, the aircraft can decelerate with a constant flight altitude or can descend without

an acceleration in its velocity. In the landing process the spoilers minimize the wing's lift, which puts more of the aircraft weight on the wheels and increases therefore the efficiency of the mechanically brakes. During the cruise flight spoilers are used in combination with ailerons to reduce the adverse yaw, if the rudder input is limited. As seen in Figure 2.1 the AC 20.30 model for the wind tunnel investigations does not exhibit spoilers, therefore the stability investigations does not consider the influences of the spoiler deflection for the lateral or longitudinal motion.

2.6 Vertical Tail Plane

The vertical tail plane (VTP) is designed to create a moment around the lateral axis, if the rudder is deflected and it ensures positive or neutral static lateral stability. The rudder is the control surface for the yaw moment, because with the rudder deflection the VTP produces a side force to compensate the yawing moments of engine failure, adverse yaw, or yaw as a result of gusts. The rudder is typically mounted on the trailing edge of the VTP fin. Deflection right pushes the tail left and causes the nose to yaw right. Centering the rudder pedals returns the rudder to neutral position and stops the yaw.

For obvious reasons the VTP airfoil has to be symmetric. The expanded tail of the BWB offers the opportunity to place a twin tail. The two planes of the twin tail have the same efficiency or even a better efficiency as the conventional configuration but with a smaller size of the two VTP's. The conventional and twin tail configuration can be examined in the Figures 2.4 and 2.5.
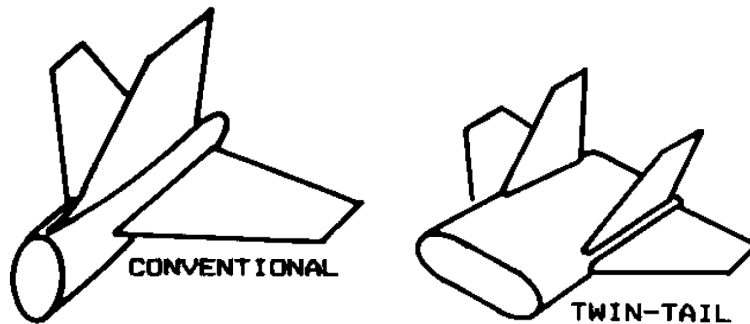
Figure 2.4: Conventional Tail (Scholz 1999)   **Figure 2.5:** Twin Tail (Scholz 1999)

24

3 The Blended Wing Body AC 20.30

3.1 The Blended Wing Body Configuration

As a result of the numerous air connections the world becomes closer and closer over the years, therefore the aircraft becomes the most important transport vehicle for medium or long range. For the prognosticated increase of the number of passengers and the rising costs for kerosene the aircraft building companies have to design large aircraft with low kerosene consumption. It can be reduced by new engines and by a reduce of the drag of the aircraft.

With the A380 Airbus arrives a barrier for conventional aircraft configurations regarding to aerodynamic efficiency and capacity, therefore aircraft building companies and aircraft research centers have started to investigate new non conventional aircraft configurations for the design of new transport aircraft.

An auspicious concept for a non conventional aircraft configuration the blended wing body turned out as a result of these researches and investigations. This configuration offers enough room in the wings to place passengers, cargo, fuel and system units, which are distributed along the span and as a result of this design the conventional fuselage is not required anymore. This leads to a decrease of the bending moment in the wing and therefore an advantageous structure weight of the BWB. Another advantage of the BWB is the smaller wetted area of the BWB compared to a same size conventional aircraft, which leads to a smaller drag of this configuration. It exists the opportunity to save 30% of the kerosene compared to todays aircraft. Another important focus of the research is the accustic behaviour of the BWB. So this configurations offers new opportunities of noise reducing compared to the conventional aircraft.

The goal for the design process was to transport about 700 passengers over great distance (long range). The result of the design goals are the Vela 1 and Vela 2 designs designed by the DLR Germany and Airbus. The further investigations executed by the HAW Hamburg are based on the Vela 2 design and the project is called AC 20.30.

3.2 Project AC 20.30

The AC 20.30 was the result of a collaboration by students of the Technical University Munich and students of the University of Applied Science Hamburg. The task of the project was to design a cabin layout with aspects in comfort, catering, apperception of the large cabin by the passengers and the evacuating of the passenger during an emergency. With the knowledge of the project and knowledge provided by Airbus was it possible to create a $3d$ model of the AC 20.30 in the CATIA environment as seen in Figure 3.1.
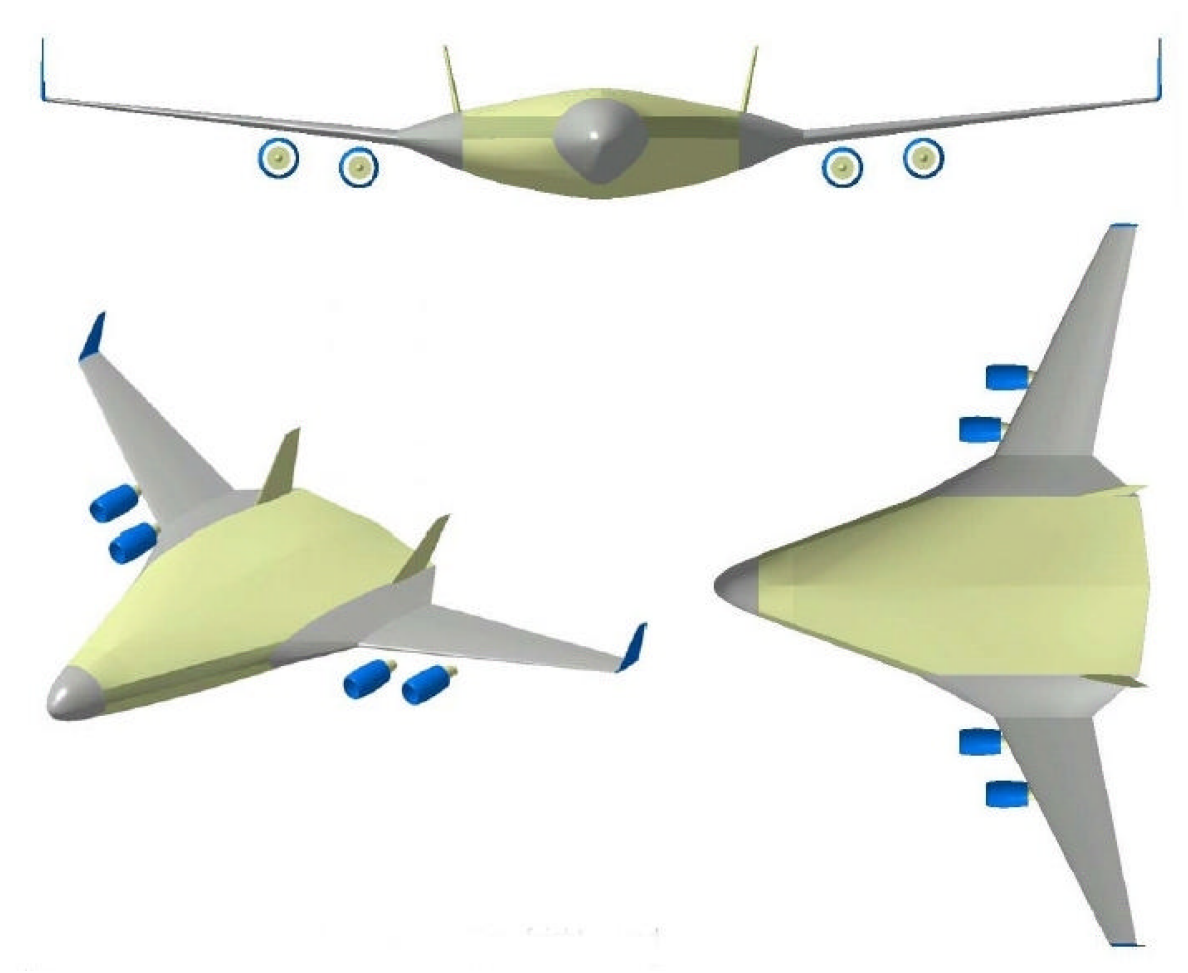
Figure 3.1: CAD-Model of the AC 20.30, Miller-Design **(Danke 2005)**

To introduce the AC 20.30 concept to the public e.g. at fairs a model of the AC 20.30 was built in a scale 1:30. The next step was to investigate the aerodynamic and flight mechanic behavior of the BWB with the help of computational fluid dynamics (CFD). After these CFD investigations were done the project group created a wireless remote

controlled AC 20.30 model in the same scale of 1:30 as the fair model to perform flight tests. The model for the flight tests can be examined in Figure 3.2. Beside CFD results wind tunnel results still are not exchangeable for aircraft design, therefore the AC 20.30 team investigated their BWB concept in the wind tunnel Dresden. It was the same model, which was used for the flight tests as seen in Figure 3.3. The computed and relevant parameters of the flight dynamic investigations are based on the results of the wind tunnel tests.

Figure 3.2: Flight Test Model **(Zingel 2006)**

Figure 3.3: Wind Tunnel Test Model **(Zingel 2006)**

3.2.1 Specification of the AC 20.30

An overview of the technical specifications of the AC 20.30 flight model is given in Table 3.1:

Table 3.1: Specification Table of the AC 20.30

Scale	$1:30$
Span	3.20 m
Length	2.12 m
Hight	0.6 m
MTOW	12.5 kg
Area Loading	6.22 kg/m^2
Engine	2 Electro Impeller
Static thrust	$22-30$ N
Cruise flight velocity	$20-30$ m/s

3.2.2 Moment of Inertia of the AC 20.30

The moment of inertia is one of the most important parameters in flight dynamics. They are the basis of the equations for the motions of the aircraft. The different moments of inertia for the AC 20.30 flight test model are referred to the principle axis system introduced in Section 4.2.1. The AC 20.30 is a symmetric geometry in the x, y-plane, therefore the moment of inertia in this plane is $I_{xy} = 0$. The other moments of Inertia are listed in the following Table 3.2 below:

Table 3.2: Moments of Inertia for the AC 20.30

I_x	5.742 kg$\times$m^2
I_y	5.98977 kg$\times$m^2
I_z	11.45476 kg$\times$m^2
I_{xz}	0.07243 kg$\times$m^2

4 Environment for the Investigations

4.1 Flight Conditions

The flight conditions for the following investigations of the aircraft stability and for the maneuver simulation are listed here in table 4.1. The flight conditions for the investigation are equal to the conditions in the wind tunnel Dresden, so the measured aerodynamic coefficients and derivatives could be used for this investigation.

<div align="center">

Table 4.1: Flight Conditions

Angle of attack α	2°
Chord line length c	1.149 m
Mach number M	0.06
Density ρ	1.225 kg/m^3

</div>

The provided aerodynamic coefficients have to be computed with linear interpolation, because in the wind tunnel not all configurations were measured for $\alpha = 2^o$. The applicatíon of the linear interpolation is useful for the aerodynamic coefficients, because for the aerodynamic coefficients as a function of α show linear behaviour for small values of α. The interval of the linear interpolation is between $[\alpha_1 = 0^o; \alpha_2 = 4^0]$.

4.2 Reference Axes Systems

4.2.1 Body Axes System

The reference axes system is fixed in the center of gravity (CG) of the aircraft and therefore it is equal to the body axes system. In Figure 4.1 the orientation of the body axes is shown, along with the nomenclature of the positive linear force (X, Y, Z), velocity (u, v, w), moment (L, M, N) and angular velocity (p, q, r) components. The body axes are very important for the flight dynamics, because they are used as the reference axes to define the equations of motion (**Nelson 1998**).
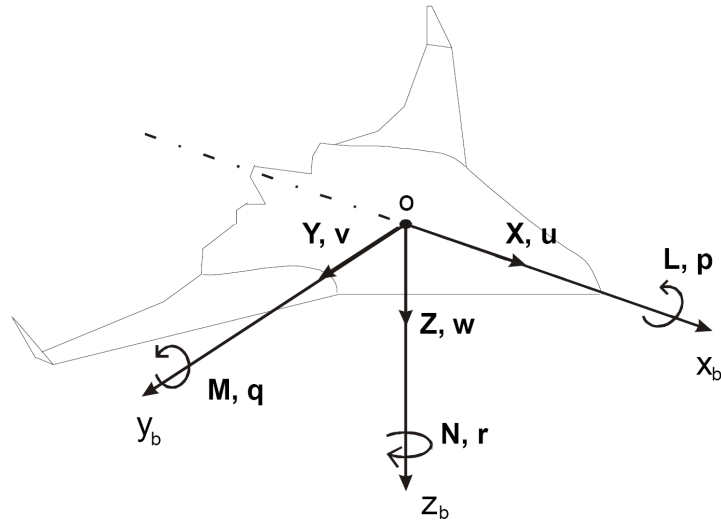
Figure 4.1: Body Axis System of the BWB(**Castro 2003**)

4.2.2 Stability Axes Sytem

The stability axes system (OX_w, Y_w, Z_w) is also known as the wind axes system in the literature. It is in symmetric flight just a particular version of the body axes system, which is rotated by the angle of attack α around the Oy_b axis as shown in Figure 4.2. It
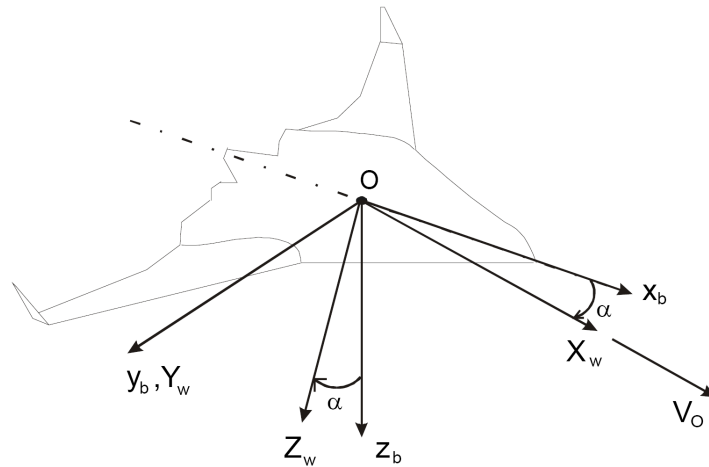
Figure 4.2: Wind Axis System of the BWB(**Castro 2003**)

has the convenience that the total velocity vector $\vec{V_0}$ is parallel to the OX_w axes. This system is often used in wind tunnel test as reference to the values of the aerodynamic lift, drag, side force.

5 The Motions of an Aircraft

5.1 Overview of the Motions of an Aircraft

As seen in Figure 5.1 an aircraft has six effective degrees of freedom in the global axis system. These six effective degrees of freedoms are the yaw moment (around the z-axis, pitch moment (around the y axis) and the roll moment (around the x-axis). The critical moments for the stability of a trimmed aircraft are the pitch and roll moment i.e. the lateral(roll) and longitudinal(pitch) motion.
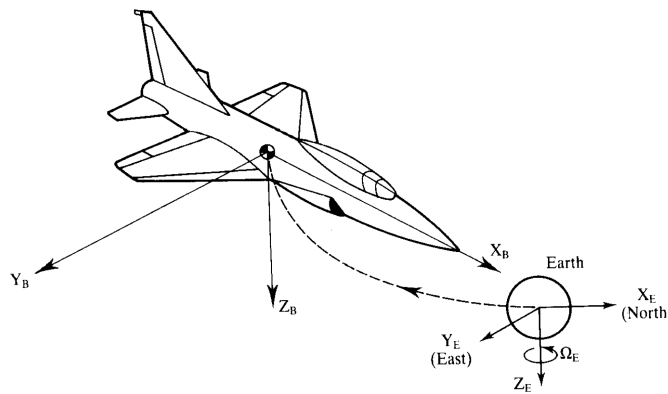
Figure 5.1: Motion of an Aircraft **(Clean 1990)**

5.2 The State Equation

A state equation is a first order vector differential equation. It represent the motion of an aircraft in natural form. So the state equation for a trimmed aircraft is defined as followed:

$$\dot{x} = A\vec{x} + B\vec{u} \tag{5.1}$$

The matrix A is the state coefficient matrix, $\vec{x}$ is the state vector, B is the driving matrix and $\vec{u}$ is the control vector. The state equation is an attractive mathematical method

to describe the control and stability of an aircraft for known inputs. Furthermore, this same form of equation lends its of to simulation.

In order to catch disturbance or atmospheric turbulence the state equation has to verify. For this content the state equation is defined as follows according to **Mc Clean 1990**:

$$\dot{x} = A\vec{x} + B\vec{u} + E\vec{d} \tag{5.2}$$

while the vector d of the dimension l represents the number of sources of the disturbances **(Clean 1990)**. The associated matrix E is of the order $(n \times l)$. Si E and d introduces the disturbances to the state equation.

However, the problem of disturbances does not appear in this thesis, therefore the state equation 5.1 is used in this thesis instead of Equation 5.2. The special methods of introducing the disturbances into the state equations can be comprehended in the literature **(Clean 1990)**.

5.3 The Output Equation

The output equation is an algebraic equation, which depends solely on the state vector $\vec{x}$ and control vector $\vec{u}$. The definition of the output equation is expressed in the following equation:

$$y = C\vec{x} + D\vec{u} \tag{5.3}$$

The out vector is $\vec{y} \in R^p$ and its elements are referred to as the output variables. The output matrix C and the feed forward matrix D are generally rectangular of the order order $p \times n$ and $p \times m$.

The C matrix determines the relationship between the system state and the system output. The D matrix allows for the system input to affect the system output directly. A basic feedback system as used in this thesis does not have a feed forward element, and therefore the D matrix is a null matrix.

5.4 Equation for the Longitudinal Motion

The state vector defines the appearance of the coefficient matrix A and the driving matrix B, therefore the state vector $\vec{x}$ has to be defined first for the longitudinal motion.

The used state vector for the following investigation of the stability behavior for the longitudinal motion is defined according to **Mc Clean 1990**:

$$\vec{x} = \begin{pmatrix} u \\ w \\ q \\ \theta \end{pmatrix} \tag{5.4}$$

The definition and the derivation of the elements of the state vector can be taken of **Mc Clean 1990**.

With the state vector mentioned in Equation 5.4 and the aircraft controlled by means of the elevator deflection (δ_E) and the flaps deflection (δ_F) the control vector is defined for the longitudinal motion as:

$$\vec{u} \triangleq \begin{pmatrix} \delta_E \\ \delta_F \\ u_g \\ w_g \\ q_g \end{pmatrix} \tag{5.5}$$

The definition of the coefficient matrix A and the driving matrix B can be seen in the following Equations 5.6 and 5.7 based on the state vector of Equation 5.4:

$$A \triangleq \begin{pmatrix} X_u & X_w & 0 & -g \\ Z_u & Z_w & U_0 & 0 \\ \tilde{M}_u & \tilde{M}_w & \tilde{M}_q & 0 \\ 0 & 0 & 1 & 0 \end{pmatrix} \tag{5.6}$$

$$B \triangleq \begin{pmatrix} X_{\delta_e} & X_{\delta_F} & -X_u & -X_w & 0 \\ Z_{\delta_e} & Z_{\delta_F} & -Z_u & -Z_w & -U_0 \\ \tilde{M}_{\delta_E} & \tilde{M}_{\delta_F} & -\tilde{M}_u & -\tilde{M}_w & -\tilde{M}_q \\ 0 & 0 & 0 & 0 & -1 \end{pmatrix} \tag{5.7}$$

A number of parameters appear frequently in the equations for defining stability derivatives for the longitudinal motion. They are listed here for convenience:

- S Area of the wing
- $\bar{c}$ mean aerodynamic chord line
- b the wing span
- m mass of the aircraft

- Aerodynamic Coefficients:
  - Pitching Moment C_m
  - Drag Coefficient for C_D
  - Lift Coefficient for C_L

5.4.1 Stability Derivatives of the Coefficient Matrix A

Force Derivatives

The u derivative of the aerodynamic forces x and z can be defined according to **Nelson 1998**:

$$X_u = \frac{\rho \cdot S \cdot u}{m} \cdot (-C_D - C_{D_u}) \tag{5.8}$$

$$Z_u = \frac{\rho \cdot S \cdot u}{m} \cdot (-C_L - C_{L_u}) \tag{5.9}$$

C_{D_u} is the derivative of the drag coefficient by the change with the forward speed as defined in Equation 5.10:

$$C_{D_u} = \frac{u}{2} \cdot \frac{\partial C_D}{\partial u} \tag{5.10}$$

and C_{L_u} is the derivative of the lift coefficient by the change with the forward speed expressed in Equation 5.11:

$$C_{L_u} = \frac{u}{2} \cdot \frac{\partial C_L}{\partial u} \tag{5.11}$$

The w derivate of the aerodynamic forces x and z can be expressed as followed:

$$X_w = \frac{-\rho \cdot S \cdot U_0}{2m} \cdot (C_{D_\alpha} - C_L) \tag{5.12}$$

$$Z_w = \frac{-\rho \cdot S \cdot U_0}{2m} \cdot (C_{L_\alpha} + C_D) \tag{5.13}$$

The drag coefficient C_{D_α} is caused by the change of the drag coefficient with the chance of the angle of attack at a constant velocity. The definition of C_{D_α} and C_{L_α} the lift curve slope can be examined in the Equations 5.14 and 5.15:

$$C_{D_\alpha} = \frac{\partial C_D}{\partial \alpha} \tag{5.14}$$

$$C_{L_\alpha} = \frac{\partial C_L}{\partial \alpha} \tag{5.15}$$

Moment Derivatives

The momentum "tilde" derivatives of the coefficient matrix A are expressed with the following three equations:

$$\tilde{M}_u = M_u + M_{\dot{w}} \cdot Z_u \tag{5.16}$$

$$\tilde{M}_w = M_w + M_{\dot{w}} \cdot Z_w \tag{5.17}$$

$$\tilde{M}_q = M_q + U_0 \cdot M_{\dot{w}} \tag{5.18}$$

The four unknown derivatives of the last equations have to be finally defined to get all necessary components of the coefficient matrix A.

The momentum derivative M_u represents the change of the pitching moment caused by a change in the forward speed, therefore the derivative depends also in the change of the Mach number, dynamic pressure or aeroelastic effects. The change in the Mach number and the aeroelastic effects have become really important for modern aircraft. The definition of M_u is represented in the following equation:

$$M_u = \frac{\rho \cdot S \cdot U_0 \cdot \bar{c}}{I_y} \cdot (C_{m_u} + C_m) \tag{5.19}$$

while C_{m_u} is the change of the pitching moment due to the change of the forward speed.

$$C_{m_u} = \frac{\partial C_m}{\partial u} \cdot \frac{U}{2} \tag{5.20}$$

M_w represents the pitching moment caused by a change in the side speed as seen in Equation 5.21:

$$M_w = \frac{\rho \cdot S \cdot U_0 \cdot \bar{c}}{2I_y} \cdot C_{m_\alpha} \tag{5.21}$$

The non dimensional stability derivative C_{m_α} is the change in the pitching moment coefficient with the angle of attack. It is referred to the longitudinal static stability derivative.

$$C_{m_\alpha} = \frac{\partial C_m}{\partial \alpha} \tag{5.22}$$

C_{m_α} is very much affected by any aeroelastic distortions of the wing, the tail and the fuselage. The stability of an aircraft is related to CG, the aerodynamic center (ac) and C_{m_α} e.g.: $x_{ac} < 0$ and C_{m_α} is negative the aircraft is statical stable, but if $x_{ac} < 0$ and C_{m_α} is positive the aircraft shows statical unstable behavior.

M_w is also related to the aircraft static margin and from these points of view M_w is the most important derivative longitudinal motion.

M_q contributes a essential part of the damping of the short period motion for the conventional aircraft and is defined according to (**Clean 1990**):

$$M_q = \frac{\rho \cdot S \cdot U_0 \cdot \bar{c}^2}{4 I_y} \cdot C_{m_q} \tag{5.23}$$

The damping results from the changes in the angle of attack of the tail. M_q is also proportional to the tail length l_t. It is the lever arm through which the lift force on the horizontal tail is convented into amount **Mc Clean 1990** i.e.:

$$M_q \propto l_t^2 \tag{5.24}$$

M_q is a very significant stability derivative, which has a primary effect on the handling qualities of the aircraft. C_{m_q} is the change of the pitching moment caused by the change in the dynamic pressure q and therefore it is defined as followed:

$$C_{m_q} = \frac{\partial M}{\partial \left(q\bar{c}/2U_0 \right)} \tag{5.25}$$

The last derivative to describe the longitudinal motion is the $M_{\dot{w}}$ and it is expressed according to **Nelson 1998**:

$$M_{\dot{w}} = \frac{\rho \cdot S \cdot \bar{c}^2}{4 I_y} \cdot C_{m_{\dot{\alpha}}} \tag{5.26}$$

The definition of $C_{m_{\dot{\alpha}}}$ is expressed as followed:

$$C_{m_{\dot{\alpha}}} = \frac{\partial C_m}{\partial \left(\alpha\bar{c}/2U_0 \right)} \tag{5.27}$$

Although $C_{m_{\dot{\alpha}}}$ does not have a powerful effect upon an aircraft's motion. But it effects significantly the short period motion. Normally the value of $M_{\dot{w}}$ is smaller than 0 and therefore it increases the damping of the short period motions.

5.4.2 Stability Derivatives of the Driving Matrix B

The driving matrix B is defined of elements by the control related derivatives of the change in the deflection of the elevator and the flaps as seen in Section 5.4 and the introduced derivatives of the longitudinal motion. The longitudinal motion derivatives are introduced in Section 5.4.1 and therefore these derivatives are not mentioned in this section. The control related derivatives of the longitudinal motion for the aerodynamic force and moments are marked with a subscript δ, which signifies any deflection caused by the elevator or flaps. The subscript δ is additional marked with an e, or a F, which implies the deflection caused by the elevator or the flaps located at the wing and at the rear end.

The control related derivatives of the aerodynamic force X caused by the deflection of the control surfaces for the longitudinal motion are expressed as follows:

$$X_\delta = \frac{\rho \cdot S \cdot U_0^2}{2m} \cdot (-C_{D_\delta}) \tag{5.28}$$

while C_{D_δ} is the change of the drag coefficient caused by the deflection of the elevator or the flaps.

$$C_{D_\delta} = \frac{\partial C_D}{\partial \delta} \tag{5.29}$$

The control related derivatives of the aerodynamic force Z produced by the deflection of the control surfaces of the longitudinal motion can be seen in Equation 5.30:

$$Z_\delta = \frac{\rho \cdot S \cdot U_0^2}{2m} \cdot (-C_{L_\delta}) \tag{5.30}$$

C_{L_δ} is the result of the change with the deflection of the flaps or the elevator.

$$C_{L_\delta} = \frac{\partial C_L}{\partial \delta} \tag{5.31}$$

The last here introduced derivative as an element for the B-Matrix is the "tilde" derivative of the change of the pitching moment (M_δ) caused by the deflection of the longi-

tudinal aircraft control surfaces (flaps, elevator). The "tilde" derivative has following definition according to **Mc Clean 1990**:

$$\tilde{M}_\delta = M_\delta + M_{\dot{w}} \cdot Z_\delta \tag{5.32}$$

The momentum derivative M_δ is expressed in the next equation:

$$M_\delta = \frac{\rho \cdot U_0^2 \cdot S \cdot \bar{c}}{I_y} \cdot C_{m_\delta} \tag{5.33}$$

As mentioned for the lift coefficient and for the drag coefficient is the pitching moment derivative C_{m_δ} the result of the deflection of the elevator or the flaps:

$$C_{m_\delta} = \frac{\partial C_m}{\partial \delta} \tag{5.34}$$

5.5 Equations for the Lateral Motion

As mentioned in Section 5.4 the appearance of the coefficient Matrix A and the driving Matrix B is defined by the state vector ($\vec{x}$). The state vector for the following investigation for the lateral motion of the BWB is defined as:

$$\vec{x} \triangleq \begin{pmatrix} \beta \\ p \\ r \\ \phi \end{pmatrix} \tag{5.35}$$

With the state vector and the aircraft controlled by the aileron and rudder the control vector ($\vec{u}$) for the lateral motion is expressed according to **Mc Clean 1990**:

$$\vec{u} \triangleq \begin{pmatrix} \delta_A \\ \delta_R \\ \beta_g \\ p_g \\ r_g \end{pmatrix} \tag{5.36}$$

Now with the introduced vectors the coefficient matrix A and the driving matrix B can be defined as shown in the equation below:

$$
A \triangleq \begin{pmatrix} Y_v & 0 & -1 & g/U_0 \\ L'_\beta & L'_p & L'_r & 0 \\ N'_\beta & N'_p & N'_r & 0 \\ 0 & 1 & 0 & 0 \end{pmatrix} \tag{5.37}
$$

$$
B \triangleq \begin{pmatrix} Y^*_{\delta_A} & Y^*_{\delta_R} & -Y_v & 0 & 1 \\ L^*_{\delta_A} & L^*_{\delta_R} & -L'_\beta & -L'_p & -L'_r \\ N^*_{\delta_A} & N^*_{\delta_R} & -N'_\beta & -N'_p & -N'_r \\ 0 & 0 & 0 & -1 & 0 \end{pmatrix} \tag{5.38}
$$

A number of parameters appear frequently in the equations for defining the stability derivatives for the lateral motion, therefore these parameters are listed here for convenience:

- S Area of the wing

- $\bar{c}$ mean aerodynamic chord line

- b the wing span

- m mass of the aircraft

- I_x moment of inertia in roll

- I_z moment of inertia in yaw

5.5.1 Stability Derivatives of the Coefficient Matrix A

The motion related parameters of the coefficient matrix A have to be defined. The first introduced coefficient of A is the lateral force derivative Y_v, which has following definition:

$$
Y_v = \frac{\rho \cdot U_0 \cdot S}{2m} \cdot C_{y_\beta} \tag{5.39}
$$

The side or lateral force Y is the result of any sideslip motion obtained from the VTP of the aircraft and it opposes the side slip motion as seen for the sideslip coefficient: i.e. $C_{y_\beta} < 0$. The sideforce coefficient C_{y_β} due to a change in the sideslip angle (β) makes a large contribution to the damping of the dutch roll mode and it is expressed according to **Nelson 1998**:

$$
C_{y_\beta} = \frac{\partial C_y}{\partial \beta} \tag{5.40}
$$

For the primed and stared stability derivatives L'_i and N'_i following definition is advised to be considered:

$$L_i' = L_i + \frac{I_{xz}}{Iz} \cdot N_i \tag{5.41}$$

$$N_i' = N_i + \frac{I_{xz}}{Iz} \cdot L_i \tag{5.42}$$

The stability derivative L_β is the change in the rolling moment due to the side slip angle β and is defined as followed:

$$L_\beta = \frac{\rho \cdot U_0^2 \cdot S \cdot b}{2I_x} \cdot C_{l_\beta} \tag{5.43}$$

The change in the value of the rolling moment coefficient with the sideslip angle C_{l_β} is called the effective dihedral. The C_{l_β} derivative is very important in studies concerned with lateral stability **(Clean 1990)**. It features the damping of both the dutch roll and the spiral mode. The derivative also affects the maneuvering capability of an aircraft, particularly when lateral control is being exercised near stall by rudder action only. For the flight dynamic small negative values of C_{l_β} are wanted, because the C_{l_β} improves the damping of the dutch roll and the spiral mode, but such values are also obtained aerodynamic difficulties, which have to be avoided.

$$C_{l_\beta} = \frac{\partial C_l}{\partial \beta} \tag{5.44}$$

The change in the yawing moment with the change in the sideslip angle is the next here introduced derivative.

$$N_\beta = \frac{\rho \cdot U_0^2 \cdot S \cdot b}{2I_z} \cdot C_{n_\beta} \tag{5.45}$$

The yawing moment coefficient with the change in the side-slip angle C_{n_β} is defined as followed:

$$C_{n_\beta} = \frac{\partial C_n}{\partial \beta} \tag{5.46}$$

C_{n_β} is referred to as the static directional or Weathercock stability coefficient **(Clean 1990)**. C_{n_β} depends upon the area of the VTP and its lever arm. The aerodynamic contribution to C_{n_β} from the VTP fin is positive, but the aircraft contribution to C_{n_β} is negative.

A positive value of C_{n_β} presumes static direction stability, therefore a negative value of C_{n_β} means static instability to the aircraft (see **Nelson 1998**). C_{n_β} introduces the natural frequency of the dutch roll mode, but it is also an important factor for introducing

the characteristics of the spiral mode stability. For good handling qualities of an aircraft C_{n_β} should be large, although such values increase the disturbance effects from side gusts.

$$L_p = \frac{\rho \cdot U_0 \cdot S \cdot b^2}{4I_x} \cdot C_{l_p} \tag{5.47}$$

The derivative L_p, mentioned in equation 5.47, describes the change of the rolling moment due to the change in the rolling velocity. The C_{l_p} derivative is referred to as the roll damping derivative and is expressed in the following equation:

$$C_{l_p} = \frac{\partial C_l}{\partial \left(\frac{pb}{2U_0} \right)} \tag{5.48}$$

On this derivative the wings have a large influence. C_{l_p} in conjunction with C_{δ_A} defines the maximum rolling velocity, which is an important flying quality. The value of C_{l_p} is always negative, the only exception is when parts of the wing are stalled then positive values may occur. The derivative of the yawing moment caused by the change of the rolling velocity is defined according to **Mc Clean 1990**:

$$N_p = \frac{\rho \cdot U_0 \cdot S \cdot b^2}{4I_z} \cdot C_{n_p} \tag{5.49}$$

The change of the yawing moment coefficient due to a change in the rolling velocity C_{n_p} is expressed as followed:

$$C_{n_p} = \frac{\partial C_n}{\partial \left(\frac{pb}{2U_0} \right)} \tag{5.50}$$

The value of C_{n_p} is for the most aircraft configurations negative, but a positive value of C_{n_p} is worthwhile, because the more negative the value of C_{n_p} is, the smaller is the damping ratio of the dutch roll mode and the greater is the side slip motion which accompanies entry to or exit from a turn.

The change in the rolling moment caused by a change in the yawing velocity is defined as:

$$L_R = \frac{\rho \cdot U_0 \cdot S \cdot b^2}{4I_x} \cdot C_{l_r} \tag{5.51}$$

The change in the rolling moment C_{l_r} coefficient due the change in the yawing velocity has a noticeable effect on the spiral mode, but it does not considerable affect the dutch

roll mode. The value of C_{l_r} should be positive but as small as possible for good spiral stability of the aircraft. It can be expressed with following equation:

$$C_{l_r} = \frac{\partial C_l}{\partial \left(\frac{rb}{2U_0} \right)} \tag{5.52}$$

The lift force produced by the wing has a large influence to the C_{l_r} derivative, but if the VTP is located either above or below the x-axis it also makes a substantial contribution to the C_{l_r} derivative.

The last introduced derivative of the coefficient Matrix A for the lateral motion is the derivative N_r, which is the change in the yawing moment due a change in the yawing velocity and is defined according to **Nelson 1998**:

$$N_r = \frac{\rho \cdot U_0 \cdot S \cdot b^2}{4I_z} \cdot C_{n_r} \tag{5.53}$$

The derivative C_{n_r} is the change in the yawing moment coefficient with a change in the yawing velocity and expressed as:

$$C_{n_r} = \frac{\partial C_n}{\partial \left(\frac{rb}{2U_0} \right)} \tag{5.54}$$

The C_{n_r} derivative is also known as the yaw damping derivative. The values of C_{n_r} are usually negative. It is the main contributor to the damping of the dutch roll mode and it also contributes to the stability of the spiral mode.

5.5.2 Stability Derivatives of the Driving Matrix B

The driving matrix B is defined by the elements of the control related derivatives, which are the results of the change in the deflection of the ailerons, spoiler or rudder. Besides the control related derivatives also already introduced motion related derivatives are an element of the driving matrix B. These elements are introduced in Section 5.5.1 and therefore these derivatives are not introduced in this section.

The control related derivatives are market with a subscript δ which implies the deflection of a control surface. The subscript δ is marked again with a subscript R, which implies rudder deflection or with a subscript A, which stands for the deflection caused by the aileron.

The first here introduced derivative is the change of the side force due to deflection of the rudder or aileron Y_δ.

$$Y_\delta = \frac{\rho \cdot U_0^2 \cdot S}{2m} \cdot C_{y_\delta} \tag{5.55}$$

The change in the side force coefficient with the rudder deflection (C_{y_R}) is an unimportant derivative, except when considering using the lateral acceleration as feedback. The change in the side coefficient caused by the deflection of the aileron C_{y_A} is for most applications in the flight dynamic negligible. The coefficient C_{y_δ} is defined as follows:

$$C_{y_\delta} = \frac{\partial C_y}{\partial \delta} \tag{5.56}$$

The introduced derivative of Equation 5.55 has to be divided by the airspeed U_0 to achieve the Y_δ^* derivative, which is an element of the driving matrix B.

$$Y_\delta^* = \frac{Y_\delta}{U_0} \tag{5.57}$$

Before introducing the control related derivatives of the rolling moment and yawing moment the transfer Equations 5.41 and 5.42 have to be used to achieve the required derivatives L_δ' and N_δ' for the driving matrix B.
The alteration in the rolling moment caused by the rudder or aileron deflection is introduced in following equation:

$$L_\delta = \frac{\rho \cdot U_0^2 \cdot S \cdot b}{2I_x} \tag{5.58}$$

The change in the rolling moment coefficient due to the rudder deflection $C_{l_{\delta_R}}$ is for the most applications in the flight dynamic for stability investigation negligible. The change in the rolling moment caused by the aileron deflection $C_{l_{\delta_A}}$ is for the lateral dynamics the most important control related stability derivative. It is particularly important for low speed flight where adequate lateral control is needed to counter asymmetric gusts which tend to roll the aircraft. The $C_{l_{\delta_A}}$ is referred to as the aileron effectiveness.

The last introduced derivative for the driving matrix B is the change in the yawing moment as a result of the rudder or aileron deflection (N_δ). The derivative N_δ is defined in Equation 5.59 as follows:

$$N_\delta = \frac{\rho \cdot U_o^2 \cdot S \cdot b}{2I_z} \cdot C_{n_\delta} \tag{5.59}$$

C_{n_δ} is defined as the change of the yawing moment coefficient due to the rudder $C_{n_{\delta_R}}$ or aileron $C_{n_{\delta_A}}$ deflection and is defined as follows:

$$C_{n_\delta} = \frac{\partial C_n}{\partial \delta} \tag{5.60}$$

43

The $C_{n_{\delta_R}}$ is referred to as rudder deflection effectiveness. The sign commitment for the rudder has following definition: If the rudder is deflected to the left, i.e $\delta_R > 0$ a negative yawing moment is created on the aircraft, i.e. $C_{n_{\delta_R}} < 0$.

If $C_{n_{\delta_A}}$ of the aircraft is greater than 0 and the pilot deflects the ailerons to produce a turn, the aircraft will yaw initially in a direction opposite to that expected **(Clean 1990)**. So C_{n_δ} is a degree of the delicacy of an aircraft for the adverse yaw. The $C_{n_{\delta_A}}$ value should be small for good lateral control.

5.6 Conversion of the Wind tunnel Data into Aerodynamic Data

5.6.1 Determination of the Aerodynamic Coefficients

It is not possible to measure the aerodynamic coefficients directly in the wind tunnel Dresden, because the used measuring equipment in the wind tunnel employs an aerodynamic scale, which measures the appeared forces in x-, y-, and z-directions and the corresponding moments. Now the required aerodynamic coefficients for the stability investigations for the longitudinal and lateral motion can be computed with the help of the in the wind tunnel measured forces and moments as seen in the following six equations:

$$C_L = \frac{F_z}{q \cdot S} \tag{5.61}$$

$$C_D = \frac{F_x}{q \cdot S} \tag{5.62}$$

$$C_y = \frac{F_y}{q \cdot S} \tag{5.63}$$

$$C_m = \frac{M_y}{q \cdot S \cdot l_m} \tag{5.64}$$

$$C_n = \frac{M_z}{q \cdot S \cdot l_m} \tag{5.65}$$

$$C_l = \frac{M_x}{q \cdot S \cdot l_m} \tag{5.66}$$

5.6.2 Determination of the Aerodynamic Derivatives

The conversions of the measured wind tunnel data sets to the aerodynamic derivatives require a plot of the measured data sets as functions of the wind tunnel settings (angle of attack α, dynamic pressure q, velocity u) or the control surface deflection δ. The result of these plots are curves, which describe the characteristics of the aerodynamic coefficients to these settings. The slopes of these plotted curves are the required aerodynamic derivatives. This method can be perfectly described on the basis of the computation of the lift curve slope:

First the lift coefficient has to be plotted as a function of the angle of attack at a constant velocity. After the curve is plotted, a linear regression of this slope has to be generated to alleviate the determination of its gradient. The gradient of the linear regression is just an approximation of the lift curve slope value, but for most wind tunnel applications this approximation is accurate enough to compute with this gradient the value of the lift curve slope. In the given example of Figure 5.2 the value of the gradient has to be multiplied with $180^o/\pi$ to change the unit from $1/[^o]$ to 1/rad.
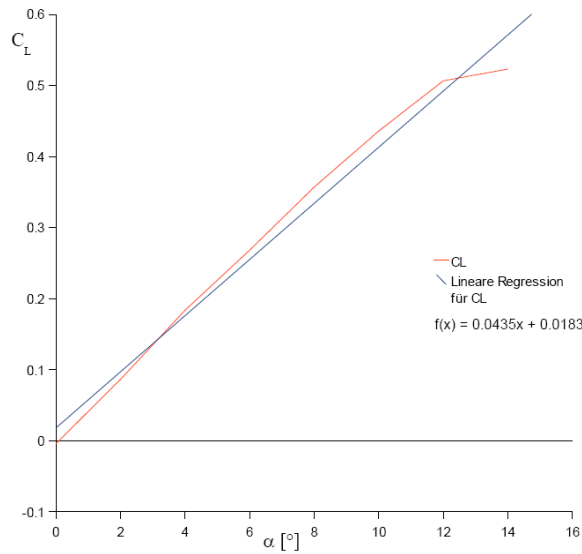
Figure 5.2: Lift Coefficient Plot including a Linear Regression

This introduced procedure can be used to determine all required aerodynamic derivatives, but different as for the determination of the aerodynamic derivatives marked with a subscript α, the aerodynamic coefficients have to be plotted as function of δ, u and q. The subscript of the derivatives defines the x-axis of the plot.

6 Introduction to the Aircraft Stability

6.1 Definition of the Stability

Stability is a property of an equilibrium state. To discus stability the meaning of the equilibrium has to be defined first. If an aircraft is to remain in steady uniform flight the resultant forces and the resultant moments about the center of gravity must be equalized to 0. An aircraft satisfying this requirement is in a state of equilibrium. The state of equilibrium is called trimmed flight in flight dynamics. The property of an aircraft to preserve the trimmed flight conditions e.g. its altitude or to resist displacements and if displaced, to develop forces and moments tending to restore the original conditions is called stability. The stability of an aircraft is divided in the static and in the dynamic stability.

6.1.1 Definition of the Static Stability

The static stability can be explained by a ball on a surface. Initially the ball is in equilibrium, then the ball experiences a displacement from the equilibrium position caused by forces or moments. The behaviour of the ball has to be observed after the ball experienced the displacement. This can be divided into three different cases:

- statically stable
- statically unstable
- neutrally stable

In the flight dynamics the statically stable and unstable cases are important, the neutrally stable case occurs rarely in the flight dynamics.

Statically Stable

After the acting of forces and moments on a body caused by a disturbance, the body tends to return immediately to its equilibrium position as seen in Figure 6.1. If the body acts like this the body is called statically stable.
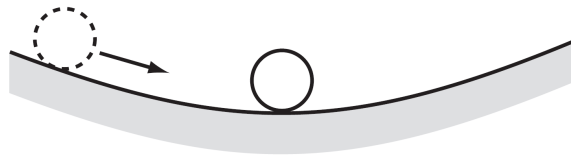
Figure 6.1: Statically stable **(Nelson 1998)**

Statically Unstable

After the acting of forces and moments on a body resulted of a disturbance, the body continues to move away from its equilibrium position as seen in Figure 6.2, then the body is defined as statically unstable.
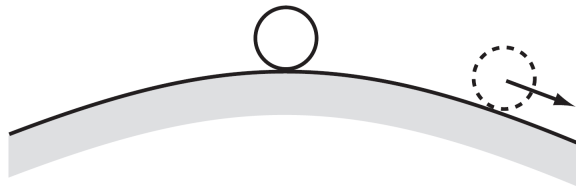
Figure 6.2: Statically unstable **(Nelson 1998)**

Neutrally Stable

If the body is disturbed but the moments remain zero the body stays in equilibrium and is neutrally stable as seen in Figure 6.3.

Figure 6.3: Neutrally stable **(Nelson 1998)**

6.1.2 Static Stability for the longitudinal Motion

The longitudinal static stability referrers to the aircraft's stability in the pitching plane. If an aircraft is longitudinal stable a small increase in the angle of attack will cause in a

change of the pitching moment, which decreases the angle of attack. On the other hand, a small decrease in the angle of attack will cause in a change of the pitching moment, which increases the angle of attack. This content can be explained with the help of Equation 6.1 for the pitching moment.

$$C_m = C_{m_0} - C_L \left(x_{cg} - x_{ac} \right) \tag{6.1}$$

This equation is derived for tailless aircraft, for trimmed equilibrium, quasi steady flight, constant mass and for small angles of attack. As seen in Equation 6.1 the pitching moment is a function of the lift coefficient (C_l), the distance of the center of gravity to aerodynamic center ($x_{cg} - x_{ac}$) and the pitching moment caused by the wing (C_{m_0}). For the Equation 6.1 the pitching moments due to the engine and the center of gravity normal displacement are neglected. Another important constraint for the longitudinal static stability is, that the derivative M_w is negative otherwise the aircraft is longitudinal static unstable.

6.1.3 Static Stability for the lateral Motion

The lateral static stability is concerned with the aircraft ability to maintain wings level equilibrium in the roll sense. The parameter with the largest influence to the lateral static stability of an aircraft is the dihedral of a wing.The dihedral effect of the tailess configuration is in the same degree as for the conventional aircraft. This parameter is the easiest way in the design process to adjust and bring the degree of lateral stability to an acceptable level. Another condition for an aircraft to be laterally stable is that the rolling moment resulting from a positive disturbance in roll direction must be negative as given in the Equations 6.2 and 6.3:

$$C_{l_\beta} = \frac{\partial C_l}{\partial \phi} < 0 \tag{6.2}$$

$$C_{l_\beta} = \frac{\partial C_l}{\partial \beta} < 0 \tag{6.3}$$

As a result of the Equation 6.3 the derivative L_β has to be negative for the lateral static stability.

6.1.4 Directional static Stability

Directional or weathercock stability deals with the static stability of an aircraft about the z-axis. As in the case for the longitudinal stability, it is desirable that the aircraft should tend to return to an equilibrium condition when it experiences a yawing disturbance. For static directional stability the aircraft must develop a yawing moment that restore

the aircraft to its equilibrium state. To develop are restoring moment to provide static directional stability the slope of the yawing moment (C_{n_β}) must be positive as seen in Equation 6.4.

$$C_{n_\beta} = \frac{\partial C_n}{\partial \beta} \; > \; 0 \tag{6.4}$$

According to Equation 6.4 the introduced motion derivative N_β has to be positive for static directional stability.

6.1.5 Function of the Stability Derivatives for the Static Stability

The stability derivatives of the lateral and longitudinal motion introduced in Sections 5.4 and 5.5 are helpful to define if an aircraft is static stable. As referred before the signs of the derivatives define if the aircraft is statically stable, therefore the signs definitions of the derivatives, which are not mentioned in the Sections 6.1.2, 6.1.3and 6.1.4 for the static stability are listed here:

- Forward speed stability X_u has to be negative
- Vertical speed stability Z_w has to be negative
- Sideslip stability Y_β has to be negative

6.2 Definition of the Dynamic Stability

The dynamic stability is concerned with the time history if the motion of the aircraft after it is disturbed from the equation point. An aircraft can be statically stable but dynamically unstable, therefore static stability does not guarantee dynamic stability.

The dynamic stability is the reduction of the disturbance with the time indicates that there is a resistance to the motion and therefore an energy dissipation. In the flight dynamic the dissipation of energy is called positive damping. If energy is added to the system it is called negative damping.

The positive damping of an aircraft is provided by forces and moments that appear caused to the aircraft motions. During positive damping these forces and moments counteracts the aircraft motions and therefore the disturbance will be damped out with time.

An aircraft that has a negative damping is dynamical unstable. For dynamically unstable aircraft artificial damping must be designed into the aircraft, which will damp out the motion. But the artificial damping does not influence the pilot control actions.

6.3 Dynamic Stability Modes for the longitudinal Motion

6.3.1 Short Period Mode

A short period oscillation is referred in the literature as the short period mode. During the short period mode the flight altitude and flight direction are constant, just the angle of attack experiences a variation. The short period mode is a very fast and heavily damped oscillation with a period of a few seconds. The motion of it is a damping about the center of gravity. The Short Period mode can be seen in Figure 6.4.
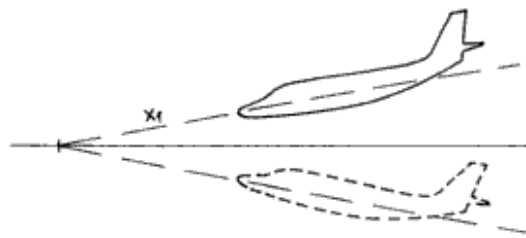
Figure 6.4: Short Period Mode Motion (**Brockhaus 2001**)

6.3.2 Phugoid Mode

The Phugoid mode is also known in the literature as long period oscillation. In the Phugoid mode there is a large amplitude variation of the aircraft velocity, pitch and flight altitude. The only constant parameter is the angle of attack. The Phugoid mode starts with a dive caused by control inputs or disturbances (e.g. gusts). The aircraft incepts itself and starts to climb again to the equilibrium position of the begin of the Phugoid mode. The climbing of an aircraft is the result of the higher velocity which the aircraft experiences during the dive. As known in the flight mechanics a higher velocity by a constant angle of attack results in a higher lift force, which leads to an increase in the flight altitude. The Phugoid mode has a lower frequency and is not this heavily damped compared to the Short Period mode. The course of motions can be examined in Figure 6.5.
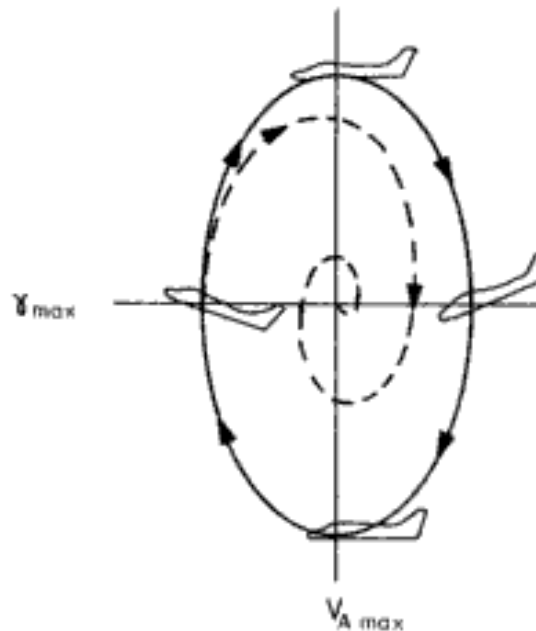
Figure 6.5: Course of Motions of the Phugoid Mode **(Brockhaus 2001)**

6.4 Dynamic Stability Modes for the lateral Motion

6.4.1 Dutch Roll Mode

The Dutch Roll is a lightly damped oscillatory motion having a low frequency. It is a combination of the yawing and rolling oscillations. The name Dutch Roll is based on the fact that this motion reminded someone of the weaving motion of a Dutch ice skater **(Nelson 1998)**.

Susceptible to this motion are aircraft with a combination of a large aft sweep angle and with a dihedral wing form. To decrease the proneness to the Dutch Roll the BWB configurations usually are usually designed with anhedral wing form. An exception for the usually BWB design is the AC 20.30. It has a large aft sweep angle and a dihedral wing configuration, therefore the AC 20.30 is very susceptible to the Dutch Roll motion. The Dutch Roll mode is visualized in Figure 6.6.
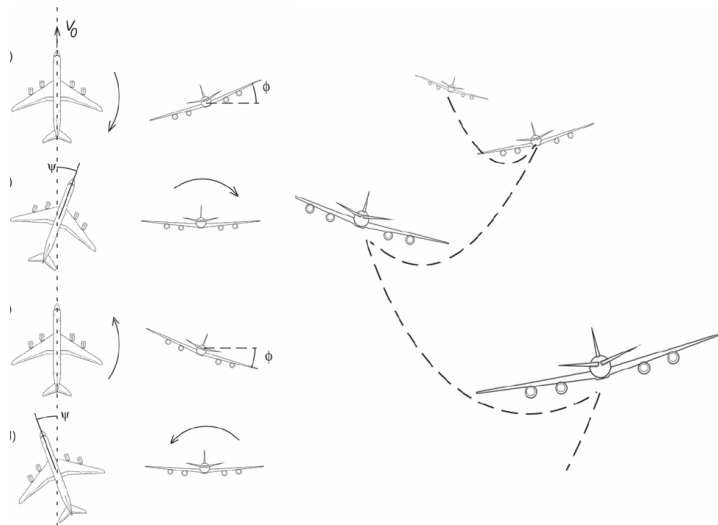
Figure 6.6: Course of Motions of the Dutch Roll Mode **(Nelson 1998)**

6.4.2 Roll Mode

The Roll mode is a highly convergent motion. It follows immediately a lateral directional disturbance and it is a heavily damped roll subsidence mode, where the aircraft experiences a motion predominantly about the body axis. During the Roll mode the
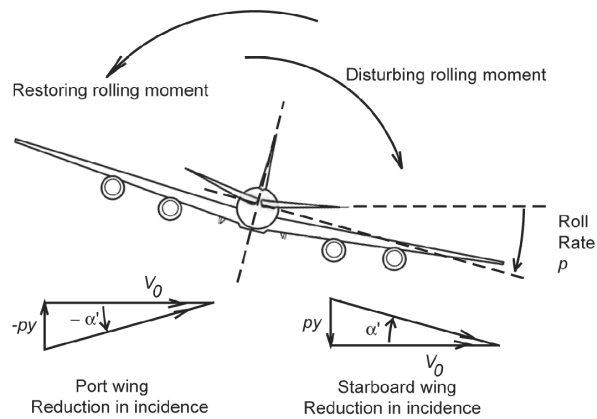
Figure 6.7: Course of Motions of the Roll Mode**(Nelson 1998)**

other variables vary slowly, hence the change of the side slip angle $\Delta\beta$, the change in in the head angle $\Delta\psi$, the roll damping r and the roll damping acceleration $\dot{r}$ can be

placed to 0. With this assumption the side force and yawing moment equations can be neglected for the Roll mode.

6.4.3 Spiral Mode

The Spiral mode is a slowly convergent or divergent motion. It is characterized by changes in the bank angle ϕ and the heading angle ψ. The side slip angle β is generally quiet small, but can not be neglected because the aerodynamic moments depend on it. The stability derivatives L_β and N_r are usually negative quantities for the most aircraft and on the other hand N_β and L_r are positive quantities for the most aircraft, therefore with this sign definition the conditions for a stable Spiral mode can be introduced according to **(Nelson 1998)**:

$$L_\beta N_r - N_\beta L_r \;>\; 0 \tag{6.5}$$

$$L_\beta N_r \;>\; N_\beta L_r \tag{6.6}$$

The aircraft behaviour, during the Spiral mode, can be examined in Figure 6.8.
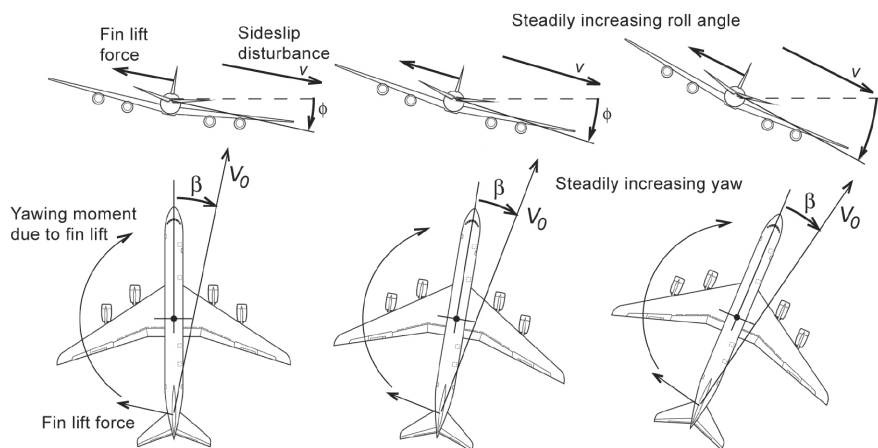
Figure 6.8: Course of Motions of the Spiral Mode**(Nelson 1998)**

6.5 Definition for the Dynamic Stability for the longitudinal Motion

The dynamic stability of the longitudinal motion can be defined with the help of the eigenvalues of the coefficient matrix A. The eigenvalues of A can be found by solving the following equation:

$$det\,|\lambda I - A| = 0 \qquad (6.7)$$

The matrix I is a 4×4 identity matrix. By solving the determinant of the Equation 6.7 the fourth degree characteristic polynomial can be expressed as follows:

$$\lambda^4 + a_1\lambda^3 + a_2\lambda^2 + a_3\lambda + a_4 = 0 \qquad (6.8)$$

The aircraft is called dynamically stable if all its eigenvalues λ_i of the coefficient matrix A for the lateral and longitudinal motions are real have negative values or if they are complex the real parts have to be negative. If the eigenvalues are zero or positive values of the real part of any complex eigenvalue then the aircraft will be dynamically unstable. In the flight dynamics it is popular to factorize the Equation 6.8 into the following equation:

$$\left(s^2 + 2\xi_{ph}\omega_{ph}s + \omega_{ph}^2\right) \cdot \left(s^2 + 2\xi_{sp}\omega_{sp}s + \omega_{sp}^2\right) = 0 \qquad (6.9)$$

The first factor of Equation 6.9 represents Phugoid mode, therefore the coefficient ξ_{ph} is the damping ratio of the Phugoid mode and ω_{ph} is the naturally undamped frequency of the Phugoid mode. The second factor of Equation 6.9 represents the Short Period mode of an aircraft, therefore the coefficients ξ_{sp} and ω_{sp} are the damping ratio and the naturally undamped frequency of the Short Period mode. These parameters can be determined with following mathematical coherence for quadratic equations. If the the quadratic equation looks like this:

$$\left(s^2 + 2\xi\omega s + \omega^2\right) = 0 \qquad (6.10)$$

the solution of the quadratic equation is given by:

$$s_{1,2} = -\sigma \pm i\omega_d \qquad (6.11)$$

while the real part σ has following definition:

$$\sigma = -\xi\omega_n \qquad (6.12)$$

The undamped naturally frequency ω_d for the Short Period mode and the Phugoid mode of the longitudinal motion can be expressed with following equation:

$$\omega_d = \omega_n \cdot \sqrt{1 - \xi^2} \tag{6.13}$$

The damping ratio ξ for both modes of the longitudinal motion is a function of the real part and the undamped naturally frequency as seen in Equation 6.14:

$$\xi = \frac{1}{\sqrt{1 + \left(\frac{\omega_d}{\sigma}\right)^2}} \tag{6.14}$$

6.5.1 The Controll Anticipation Parameter

The control anticipation parameter (CAP) is based on the consideration of the pilot comments and the physiology of the pilot. The CAP is the ratio of the instantaneous angular acceleration in the pitch direction to the steady state change in the load factor, when the longitudinal control inputs are done by the pilot. The CAP is a function of the naturally frequency of the Short period mode ω_{sp} and the acceleration sensitivity $n_{z\alpha}$ as seen in Equation 6.15:

$$\text{CAP} = \frac{\omega_{sp}^2}{n_{z\alpha}} \tag{6.15}$$

The acceleration sensitivity is defined with following equation:

$$n_{z\alpha} = \frac{-U_0}{g \cdot Z_w} \tag{6.16}$$

The theoretical background of the CAP method is that in order to make defined adjustments to the flight path, the pilot must infer from the initial attitude of the aircraft, the ultimate response to the flight path **(Reichert 1987)**. The best way for sensing the attitude response is the initial angular acceleration in pitch direction, which the pilot senses through his inner ear. The value of the CAP has a main influence to the definition of the handle qualities of an aircraft. If the CAP value is too small the angular acceleration in pitch is below the threshold of the pilot inner ear **(Reichert 1987)**. If its value is too large the pilot tends to undershoot the desired flight path corrections, because any slight pitch control input generates a large angular acceleration in the pitch direction, therefore the pilot tends to reduce the pitch control input.

6.6 Definition for the Dynamic Stability for the lateral Motion

As for the longitudinal motion for the characteristic polynom of the coefficient matrix A has to be defined according to **Mc Clean 1990**:

$$det\,[\lambda I - A] = 0 \tag{6.17}$$

$$\lambda^5 + d_1\lambda^4 + d_2\lambda^3 + d_4\lambda^2 + d_4\lambda = 0 \tag{6.18}$$

The fifth degree polynom of Equation 6.18 can be factorized as followed:

$$\lambda\,(\lambda + e)\,(\lambda + f)\,\left(\lambda^2 + 2\xi_D\omega_D + \omega_D^2\right) = 0 \tag{6.19}$$

The single term λ of the Equation 6.19 corresponds to the Directional mode. For the characteristic equation $\lambda = 0$ is a root, which defines the aircraft as neutrally stable for the Directional mode as mentioned in Section 6.5. The term $(\lambda + e)$ agrees with the convergent/divergent spiral mode and the term $(\lambda + f)$ corresponds to the Roll mode. The last term of the Equation 6.19 represents the Dutch Roll mode. The coefficient ξ_D is the value for the damping ratio and is usually small, which leads the Dutch Roll to an oscillated rolling motion. The coefficient ω_D is the naturally frequency of the Dutch Roll. Different as for the longitudinal motion the naturally frequency of the Dutch Roll mode is computed with the help of the stability derivatives N'_β, N'_r and Y_v as seen in Equation 6.20.

$$\omega_D = \sqrt{N'_{beta} + N'_r \cdot Y'_v} \tag{6.20}$$

Now with the help of the naturally frequency introduced in Equation 6.20 and the stability derivatives N'_r and Y_v the damping ratio for the Dutch Roll can be defined as seen in following equation:

$$\xi_D = \frac{N'_r + Y_v}{2\omega_D} \tag{6.21}$$

For the stability investigation of the Roll mode the Roll Damping Time $T_{\xi\,R}$ with the following here introduced method, if λ_3 is the eigenvalue of the Roll:

$$T_{\xi\,R} = \frac{-1}{\lambda_3} \tag{6.22}$$

The last required computed value for a successful stability investigation is the Time to Double T_s of the Spiral Mode. It can be computed with the help of the eigenvalue, which

belongs to the Spiral mode. For the coefficient matrix used in this thesis the eigenvalue λ_4 belongs to the Spiral mode and with this informations T_s can be computed with the following here introduced equation:

$$T_s = \frac{log(2)}{\lambda_4} \tag{6.23}$$

6.7 S-Plane Diagram
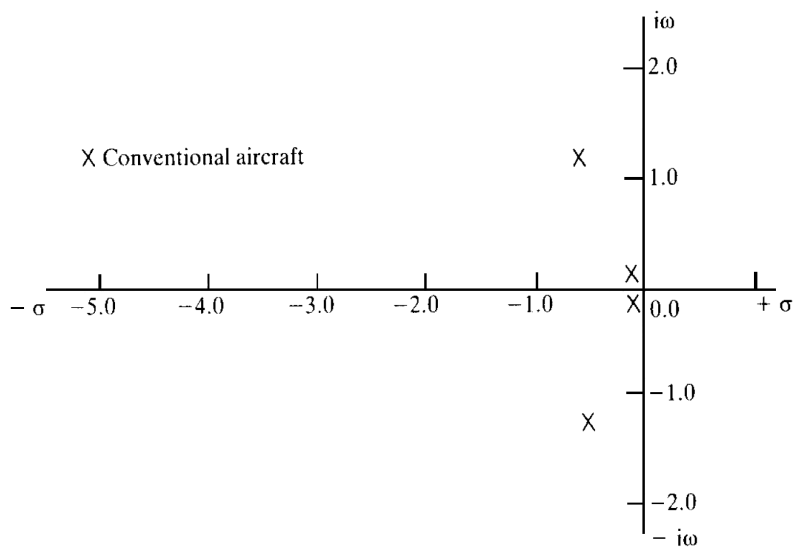
Figure 6.9: S-Plane Diagram

The location of the eigenvalues in the complex frequency environment is often shown through the s-plane diagram. A s-plane diagram with the locations of the eigenvalues for a typical conventional aircraft is shown in Figure 6.9. It is an important method to show the sensibility of the aircraft stability derivatives. With the help of this method the behavior of the eigenvalues in the s-plane can be shown as the values for the stabilities derivatives have changed.

6.8 Flight Quality

The aircraft designer is faced with the challenge of providing an aircraft with optimal performance, so that the aircraft is safe and easy to fly. To realize such a goal, the designer must know what degree of stability and control is required for the pilot to keep

the aircraft flyable and safe. So the flying qualities of an aircraft are related to the stability and control characteristic but based on the pilot impressions. The Department of Defense of the USA and the FAA published a list of specifications dealing with the aircraft flying qualities. These requirements are used by the procuring and regulating agencies to define whether the aircraft acceptable for certification. The expected flying qualities by the pilot depend on the type of aircraft and the flight phase.

Table 6.1: Classification of Aircraft **(Nelson 1998)**

Class I:	Small, light airplanes, such as light utility, primary trainer and light observation craft
Class II:	Medium-weight, low to medium maneuverability airplanes, such as heavy utility/search and rescue or medium transport/cargo/tanker
Class III:	Large heavy, low to medium maneuverability airplanes, such as heavy bomber and trainer for Class III
Class IV:	High maneuverability airplanes such as fighter/interceptor, attack, tactical reconnaissance, observation and trainer for Class IV

The first classification according to size and maneuverability is shown in Table 6.1. The flight phase is divided into three categories as seen in Table 6.2. The category A deals exclusively with the military aircraft, while most of category B and C flight phases deal for civil and military aircraft. So the flying qualities of an aircraft are defined into three levels according to (**Nelson 1998**) can be seen in Table 6.3.

Table 6.2: Flight Phase Categories (**Nelson 1998**)

Category A:	Nonterminal flight phase, that required rapid maneuvering precision tracking, or precise flight patch control. Included in the category are air to air combat, ground attack, weapon delivery /launch, aerial recovery, reconnaissance, in-flight refuelling (receiver), terrain-following, antisubmarine search, and close-formation flying
Category B:	Nonterminal flight phases, that are normally accomplishes using gradual maneuvers and without precision trackling, although accurate flight-path control may be required. Included in the category are climb, cruise, loiter, in-flight refueling (tanker), descent, emergency descent, emergency deceleration, and aerial delivery.
Category C:	Terminal flight phase are normally accomplishes using gradual maneuvers and usually require aircraft flight path control. Included in this category are take off, catapult take off, approach, wave-off/go around and landing

The levels are based as mentioned before of the pilot's opinions of the flying characteristics of the aircraft. As mentioned before, the flying qualities of an aircraft are related to the dynamic and control characteristics of an aircraft. So the damping ratio and frequency of the Short Period mode and Phugoid mode are parameters to describe the behaviour of the dynamic and control characteristics of an aircraft and therefore these parameters can be used to define the flight qualities of an aircraft. The values in the following tables are empirical values and they are based on results during flight tests.

Table 6.3: Flight Phase Levels (**Nelson 1998**)

Level 1:	Flying qualities adequate for the mission flight phase
Level 2:	Flying qualities adequate to accomplish the mission flight phase but with some increase in pilot workload and/or degradation in mission effectiveness or both.
Level 3:	Flying qualities such that the airplane can be controlled safely but the pilot workload is excessive and/or mission effectiveness is inadequate or both. Category A flight phase can be terminated safely and Category B and C flight phase can be completed.

6.8.1 Empirical Values of the Flight Qualities for the longitudinal Motion

The Table 6.4 shows the values for the Phugoid to divide the aircraft into different flight qualities level. The Table 6.5 shows the empirical values for the damping ratio of the

Table 6.4: Flying Qualities for the Phugoid Mode (**Nelson 1998**)

Level 1:	$\xi_{ph} > 0.04$
Level 2:	$\xi_{ph} > 0$
Level 3:	$T_2 = 33$ s

Short Period mode ξ_{sp} to define the different flight quality levels.

Table 6.5: Flying Qualities for the Short Period Mode (**Nelson 1998**)

Level	Categories A and C $[\xi_{sp}]$	Category B $[\xi_{sp}]$
1	$0.35 - 1.30$	$0.3 - 2.0$
2	$0.25 - 2.00$	$0.2 - 2.0$
3	0.15	0.15

While Figure 6.10 helps to classify the CAP values of the investigated aircraft (category B flight phase) into the flight quality levels.
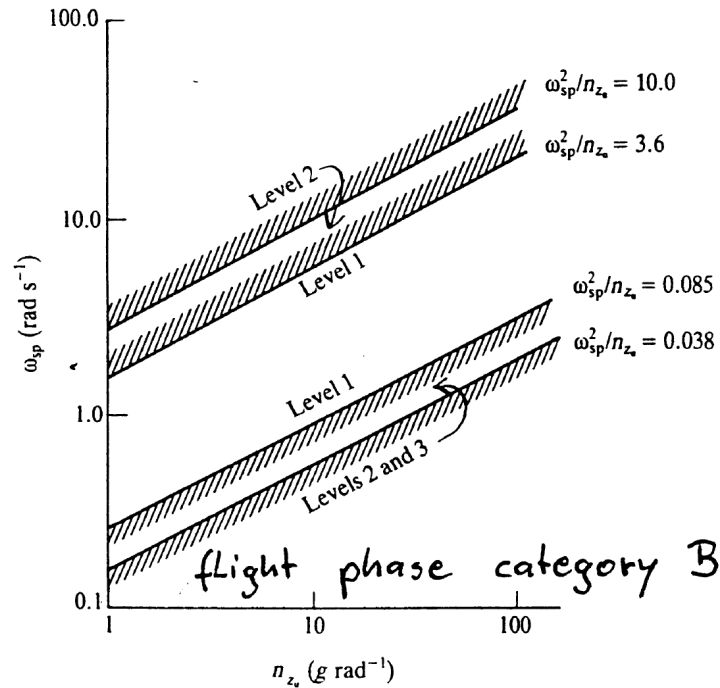
Figure 6.10: Chart of the CAP Flight Quality Level Definition for a Category B Flight Phase (**Scholz 1999**)

6.8.2 Empirical Values of the Flight Qualities for the lateral Motion

For the characteristic modes of the lateral motion are also empirical values based on the pilot opinions are used for describing the flying qualities of an aircraft. The Table 6.6 helps to divide the aircraft into the flying quality levels for the Spiral mode with the help of the the minimum time to double amplitude. The Table 6.7 helps to divide the

Table 6.6: Spiral mode minimum Time to Double Amplitude **(Nelson 1998)** Flying Qualities

Class	Category	Level 1	Level 2	Level 3
I and IV	A	12.0 s	12.0 s	4.0 s
	B and C	20.0 s	12.0 s	4.0 s
II and III	All	20.0 s	12.0 s	4.0 s

flying qualities for the Roll mode of an aircraft into the different flying qualities levels. The classification takes places with the help of the maximum roll time constant for the different aircraft classes and categories. The Table 6.8 helps to divide the aircraft into the different flight qualities of the Dutch Roll mode.

Table 6.7: Roll Mode (maximum Roll Time constant) flying Qualities **(Nelson 1998)**

Class	Category	Level 1	Level 2	Level 3
I and IV	A	1.0 s	1.4 s	10 s
II and III	A	1.4 s	3.0 s	10 s
All	B	1.4 s	3.0 s	10 s
I and IV	C	1.0 s	1.4 s	10 s
II and III	C	1.4 s	3.0 s	10 s

Table 6.8: Dutch Roll flying Qualities **(Nelson 1998)**

Level	Category	Class	Min ξ_D	Min $\xi_D\omega_D$	
1	A	I, IV	0.19	0.35 rad/s	1.0 rad/s
		II, III	0.19	0.35 rad/s	0.4 rad/s
1	B	All	0.08	0.15 s/rad	0.4 rad/s
1	C	I, II-C	0.08	0.15 rad/s	1.0 rad/s
1	C	II-L, III	0.08	0.15 rad/s	0.4 rad/s
2	All	All	0.02	0.05 rad/s	0.4 rad/s
3	All	All	0.02	−	0.4 rad/s

7 Stability Investigation for the AC 20.30

7.1 Stability for the longitudinal Motion

7.1.1 Definition of the Coefficient Matrix A for the longitudinal Motion

Aerodynamic Coefficients and Derivatives

Before the matrix A can be defined the stability derivatives for the AC 20.30 has to be determined. The aerodynamic coefficients and their derivatives for the longitudinal motion are provided by **Zingel 2006** and they are listed in the following Table 7.1:

Table 7.1: Aerodynamic Coefficients and Derivatives for the longitudinal Motion

C_l	0.175075
C_{l_α}	2.4924 rad^{-1}
C_{l_u}	-0.0040
C_D	0.0294
C_{D_α}	0.6073 rad^{-1}
C_{D_u}	-0.0040
C_m	0.0244
C_{m_α}	-0.1547 rad^{-1}
C_{m_q}	$-1 \cdot 10^{-5}$
C_{m_u}	-0.0020

Stability Derivatives

With the help of the aerodynamic coefficients, derivatives and the definition of the stability derivatives in Section 5.4.1 the elements of the coefficient matrix A can be determined as seen in the following Table 7.2. The tilde derivatives introduced in Section

5.4.1 are neglected and therefore not mentioned in Table 7.2. They are neglected, because the $C_{m_{\dot{\alpha}}}$ of the AC 20.30 defined in Equation 5.27 was not measured during the wind tunnel tests in Dresden and therefore this parameter was not provided by Till Zingel. Instead of the tilde stability derivatives the moment stability derivatives are used for the coefficient matrix A.

Table 7.2: Coefficients for the Coefficient Matrix A

X_u	-0.1037 s^{-1}
X_w	-0.8824 s^{-1}
Z_u	-0.6984 s^{-1}
Z_w	-5.1478 s^{-1}
M_u	$0.2188 \text{ m}^{-1}\text{s}^{-1}$
M_w	$-0.7572 \text{ m}^{-1}\text{s}^{-1}$
M_q	$-2.81 \cdot 10^{-5} \text{ s}^{-1}$

Coefficient Matrix A of the longitudinal Motion

According to Section 5.4 with the help of the stability derivatives the coefficient matrix A for the longitudinal motion of the AC 20.30 is defined as follows:

$$A \triangleq \begin{pmatrix} -0.1037 & -0.8824 & 0 & -9.81 \\ -0.6984 & -5.1478 & 20 & 0 \\ 0.2188 & -0.7572 & -2.81 \cdot 10^{-5} & 0 \\ 0 & 0 & 1 & 0 \end{pmatrix} \tag{7.1}$$

7.1.2 Static Stability for the AC 20.30 for the longitudinal Motion

The static stability of the AC 20.30 can be defined with the help of the stability derivatives mentioned in Section 6.1.2. The static stability for the longitudinal motion for the AC 20.30 is given because the stability derivative M_w has a negative value as seen in Table 7.2. The forward speed stability of the AC 20.30 is given as well, because as seen in Table 7.2 the X_u stability derivative has a negative sign, which defines stability according to Section 6.1.5. The vertical speed stability is also given, because the Z_w derivative does also have a negative value.

7.1.3 Dynamic Stability for the AC 20.30 for the longitudinal Motion

To investigate the dynamic stability of the AC 20.30 for the longitudinal motion the coefficient matrix A is used. The two main stability modes for the longitudinal motion are the Short Period and the Phugoid mode. The informational parameters for the dynamic stability are the eigenvalues of the coefficient matrix A. To calculate these eigenvalues the characteristic polynom of the coefficient matrix A has to be defined as seen in Equation 7.2.

$$\lambda^4 + 5.2515\lambda^3 + 15.0621\lambda^2 + 7.5793\lambda + 16.2394 = 0 \tag{7.2}$$

Now with the help of the characteristic polynom it is not a problem to compute the eigenvalues of the coefficient matrix A. These eigenvalues for Equation 7.2 have following values:

$$\lambda_1 = -2.5768 + 2.5885i$$
$$\lambda_2 = -2.5768 - 2.5885i$$
$$\lambda_3 = -0.0489 + 1.1022i$$
$$\lambda_4 = -0.0489 - 1.1022i$$

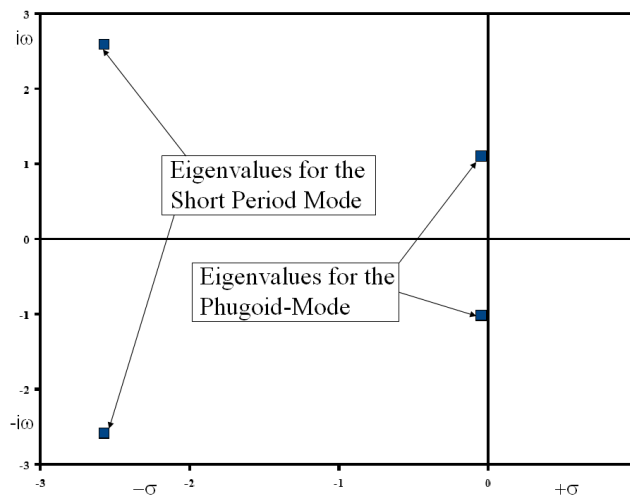**S-Plane for the longitudinal Motion of the AC 20.30**

Figure 7.1: S-Plane Diagram for the longitudinal Motion of the AC 20.30

64

The S-plane diagram is helpful to analyse the stability of an aircraft with just one look to the plot and assign the eigenvalues to the different modes. In the S-Plane diagram it can be seen that the AC 20.30 is for both important longitudinal modes are stable, because both values are located on the left side of the S-plane as seen in Figure 7.1.

Short Period Mode

The eigenvalues λ_1 and λ_2 belong to the Short Period mode as mentioned in Section 6.5. In case of the negative real parts of the eigenvalues λ_1 and λ_2 the AC 20.30 is stable in the Short Period mode.
The factorization of the Equation 7.2 leads to the characteristic equation for the Short Period mode which is mentioned here:

$$\lambda^2 + 5.15362\lambda + 13.3404 = 0 \tag{7.3}$$

With the help of the Equation 7.3 the frequency and the damping ratio of the Short Period mode for the AC 20.30 can be found with the methods introduced in Section 6.5. So these methods lead to following result for the frequency of the Short Period mode:

$$\omega_{sp} = 3.6524 \text{ rad} \cdot \text{s}^{-1}$$

The damping ratio can be computed with the same methods as the frequency and this leads to following result for the damping ratio of the AC 20.30:

$$\xi_{sp} = 0.7055$$

The positive value of the damping ratio leads to an increase of the damping, so the AC 20.30 is able to damp out the Short Period mode out external control inputs.

Phugoid Mode

The eigenvalues λ_3 and λ_4 belong to the Phugoid mode, therefore it can be seen that the aircraft is stable for the Phugoid mode. For the Phugoid mode the characteristic equation has to be designated to receive the frequency and the damping ratio of the Phugoid mode.

So with the introduced methods of Section 6.5 the frequency and the damping ratio for the AC 20.30 can be computed. But before it takes place the characteristic equation for

the Phugoid mode has to be defined, which is the second term of the factorisation of the Equation 7.2.

$$\lambda^2 + 0.0975\lambda + 1.2179 = 0 \tag{7.4}$$

So with the help of the characteristic equation following values for the frequency and damping ratio of the AC 20.30 can be computed:

$$\omega_{ph} = 1.1033 \ \ \text{rad} \cdot \text{s}^{-1}$$

$$\xi_{ph} = 0.0444$$

So the positive damping ratio shows that the AC 20.30 is able to damp out the Phugoid mode by itself without the help of external control inputs and brings the aircraft back to a stable longitudinal position.

The Control Anticipation Parameter of the AC 20.30

With the help of stability derivative Z_w, g and U_0 the acceleration sensitivity $n_{z\alpha}$ can be defined which leads to following value of it:

$$n_{z\alpha} = 10.495$$

So with the known acceleration sensitivity and the naturally frequency of the Short Period mode the CAP value can be computed.

$$\text{CAP} = 1.2711 \ \text{s}^{-2}$$

The value of CAP is flight quality level 1 value for class A aircraft (see Figure 6.10).

Flight Quality for the longitudinal Motion of the AC 20.30

With the computed values of the damping ratio and the frequency for the longitudinal motion the flight qualities of the AC 20.30 can be divided into flight quality levels according Table 6.3. But before the aircraft has to be divided into flight quality level, the aircraft has to be categorized according to Table 6.2. The AC 20.30 is a category B class III aircraft and therefore the the results has to be squared with the classifications

values of the Tables 6.4 and 6.5 for a category B aircraft. The characteristic values for the classification is the damping ratio of the Short Period mode and of the Phugoid mode.

Both values of the AC 20.30 are accomplishing the requirements for the level 1 definition for the flying qualities for the longitudinal motion as seen by comparing the computed values with the given values of the Tables 6.4 and 6.5 for the longitudinal motion.

7.2 Stability for the lateral Motion

7.2.1 Definition of the Coefficient Matrix A

Aerodynamic Coefficients and Derivatives

So before the coefficient matrix A and the stability derivatives can be defined, the aerodynamic coefficients and their derivatives for the lateral motion of the AC 20.30 have to be assigned. The Table 7.3 shows the aerodynamic coefficients and derivatives which are provided by Till Zingel.

Table 7.3: Aerodynamic Coefficients and Derivatives for the lateral Motion (**Zingel 2006**)

C_{y_β}	-0.2833 rad^{-1}
C_{l_β}	-0.1031 rad^{-1}
C_{n_β}	0.0344 rad^{-1}

But for the complete definition of all used stability derivatives for the lateral motion there are still some parameters missing according to Section 5.5.1. It was not possible to measure the missing parameters during the wind tunnel tests in Dresden, therefore this parameters are assigned by **Castro 2003**. The two BWB configurations are nearly familiar and therefore the values for the missing parameters could be taken out of Castro's thesis.

Table 7.4: Aerodynamic Coefficients and Derivatives for the lateral Motion (**Castro 2003**)

C_{l_p}	-0.2180 rad^{-1}
C_{l_r}	-0.0731 rad^{-1}
C_{n_p}	-0.0328 rad^{-1}
C_{n_r}	-0.1160 rad^{-1}

Stability Derivatives

Now with the help of the aerodynamic derivatives and coefficients the stability derivatives for the lateral motion can be defined as seen in Table 7.5:

Table 7.5: Stability Derivatives for the lateral Motion

Y_v	$-0.5783\ \mathrm{m\cdot s^{-2}}$
L_β	$-29.6983\ \mathrm{s^{-2}}$
N_β	$4.9624\ \mathrm{s^{-2}}$
L_p	$-5.0849\ \mathrm{s^{-1}}$
N_p	$-0.3835\ \mathrm{s^{-1}}$
L_r	$1.7051\ \mathrm{s^{-1}}$
N_r	$-0.1356\ \mathrm{s^{-1}}$

But for the coefficient matrix A for the lateral motion the primed derivatives have to be computed. This takes place with the help of the Equations 5.41 and 5.42 of Section 5.5.1. The primed stability derivatives have following values:

Table 7.6: Primed Stability Derivatives for the lateral Motion

L'_β	$-29.6672\ \mathrm{s^{-2}}$
N'_β	$4.7746\ \mathrm{s^{-2}}$
L'_p	$-5.0875\ \mathrm{s^{-1}}$
N'_p	$-0.4157\ \mathrm{s^{-1}}$
L'_r	$1.7042\ \mathrm{s^{-1}}$
N'_r	$-0.1248\ \mathrm{s^{-1}}$

Coefficient Matrix A of the AC 20.30 for the lateral Motion

Now with the help of the primed stability derivatives the coefficient matrix A for the lateral motion of the AC 20.30 can be set with values. The coefficient matrix A has then following appearance according to Section 5.5:

$$A \triangleq \begin{pmatrix} -0.5783 & 0 & -1 & 0.4905 \\ -29.6669 & -5.0873 & 1.7042 & 0 \\ 4.7746 & -0.4157 & -0.1249 & 0 \\ 0 & 1 & 0 & 0 \end{pmatrix} \tag{7.5}$$

7.2.2 Static Stability for the lateral Motion of the AC 20.30

The static stability for the lateral motion can be investigated with the help of the stability derivative L_β, which has to be negative for a stable behaviour of the aircraft. The AC 20.30 accomplishes the given requirement as seen in Table 7.5.

The AC 20.30 is also static stable for the directional mode, because N_β derivative is positive. This can be seen in Table 7.5 as well.

The last here investigated static stability is the side slip stability with the help of the stability derivative Y_β. This derivative is a function of the C_{y_β} coefficient derivative and as seen in Table 7.3 the C_{y_β} value is negative and therefore the AC 20.30 is static stable in the side slip motion.

7.2.3 Dynamic Stability for the AC 20.30 for the lateral Motion

The investigation of the dynamic stability of the AC 20.30 for the lateral motion the coefficient matrix A has to be used. For the lateral motion of an aircraft there are three main stability modes. These modes are the Dutch Roll mode, Spiral mode, and the Roll mode.

As for the longitudinal motion the eigenvalues of the coefficient matrix A have to be computed. To compute the eigenvalues the characteristic polynom for the lateral motion of the AC 20.30 have to be defined. It has following definition for the lateral motion:

$$\lambda^4 + 5.7904\lambda^3 + 9.1323\lambda^2 + 51.9455\lambda - 2.1744 = 0 \tag{7.6}$$

Different as mentioned in Section 6.6 the characteristic polynom for the lateral motion is a fourth degree polynom, therefore $\lambda = 0$ is not a root of the Equation 7.6. This leads to the already mentioned conclusion that the AC 20.30 is stable for the directional mode. So the eigenvalues for the lateral motion are:

$$\lambda_1 = -0.0273 + 3.0097i$$
$$\lambda_2 = -0.0273 - 3.0097i$$
$$\lambda_3 = -5.7774$$
$$\lambda_4 = 0.0415$$

All eigenvalues for the lateral motion besides λ_4 are dynamically stable, because they have negative eigenvalues.

S-Plane for the lateral Motion

With the help of the s-plane diagram (Fig. 7.2) of the lateral motion the eigenvalues of the coefficient matrix A can be assigned to the different modes for the lateral motion. So the assigned eigenvalues for the Dutch Roll mode are the eigenvalues λ_1 and λ_2. The assigned eigenvalue for the Roll mode is the eigenvalue λ_3 and the last eigenvalue λ_4 belongs to the Spiral mode.
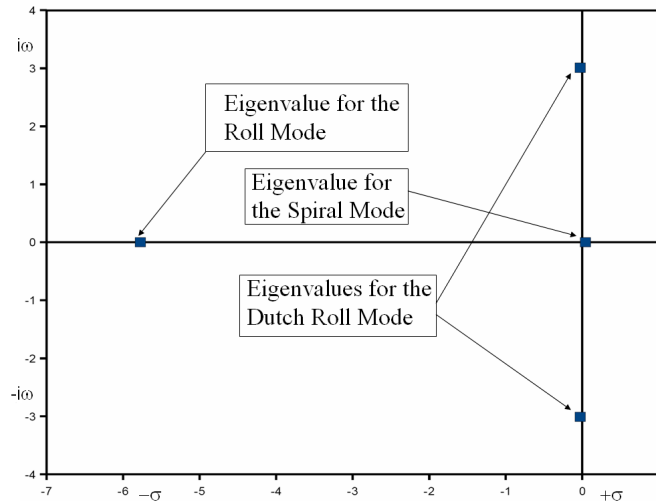

Figure 7.2: S-Plane Diagram for the lateral Motion of the AC 20.30

Stability in the Dutch Roll Mode

The eigenvalues λ_1 and λ_2 belong to the Dutch roll mode of the AC 20.30. The real parts of these eigenvalues are negative, which leads to the conclusion that the AC 20.30 is stable for the Dutch roll mode and is able to damp disturbances without external control inputs. To visualize this, the characteristic equation for the Dutch Roll mode of the AC 20.30 has to be defined. It has following appearance due to the factorisation of the characteristic polynom of the coefficient matrix A (Equation 7.6):

$$s^2 + 0.0546s + 9.0593 = 0 \qquad (7.7)$$

With the help of the Equations 6.20 and 6.21 the naturally frequency ω_D and the damping ratio ξ_D for the Dutch Roll mode can be computed with the following results:

If the investigated aircraft experiences the Dutch Roll, it can damp it out by itself, because the ξ_D value is positive.

$$\omega_D = 2.2015 \text{ rad} \cdot \text{s}^{-1}$$
$$\xi_D = 0.1597$$

Stability in the Roll Mode

The eigenvalue λ_3 belongs to the Roll mode. The λ_3 eigenvalue is real and negative, which leads to the conclusion that the AC 20.30 is stable for the Roll mode. For the flight quality investigation the roll damping time is required. The computation of it brings up following value:

$$T_{\xi_R} = 0.1731 \text{ s}$$

So the AC 20.30 is able to damp out the roll mode without external control inputs.

Stability for the Spiral Mode

The last eigenvalue (λ_4) belongs to the Spiral mode. The value of λ_4 is real but positive, this leads to the conclusion that the AC 20.30 is unstable in the Spiral mode, so the aircraft needs external control inputs to stabilize the aircraft, while the aircraft is caught in the Spiral mode. For flight qualities the time to double T_s has to be computed for the investigated aircraft. It has following value:

$$T_s = 16.6847 \text{ s}$$

Flight Quality for the lateral motion of the AC 20.30

For the lateral motion is it important to define the class of the investigated aircraft. The classification of the aircraft is introduced in Table 6.1. The AC 20.30 is a class III aircraft and the nonterminal flight phase of this aircraft is category B of Table 6.2. Now with the help of the Dutch Roll frequency and its damping, the Roll mode time constant and the time to double the flight qualities of the AC 20.30 can be determined.

For the Spiral mode the AC 20.30 shows with the computed values a level 2 behaviour according to Table 6.6. The roll time constant $T_{\xi_R} = 0.1731$ s is smaller than the 1.4 s (see Table 6.7), which is the required maximum for level 1, therefore the AC 20.30 shows for the roll mode level 1 flying qualities.

The damping of the Dutch Roll is level 1 according to the value of $\xi_D = 0.0304$ and Table 6.8. The product of the naturally frequency and the damping results in a level

1 value, because the product $\xi_D \omega_D = 0.3516$ rad$\cdot$s^{-1}, which is greater as the required value for level 1 (0.15 rad$\cdot$s^{-1}) as seen in Table 6.8. The flight quality of the naturally frequency is also level 1 and therefore the flight quality for the whole Dutch Roll mode is level 1.

8 Computational Simulation for the Motions of the AC 20.30

8.1 Flow Chart

The computational simulations for the lateral and longitudinal motions take place in the Matlab Simulink environment. But before the simulations can be designed it is advisable to design a flow chart of the simulation program to visualize the structure of the program. It is a usual method in the computer science to use the flow chart as a structure tree. Besides this it helps also to ascertain which input and state variables have to be defined to run this program. A flow chart of a simulation process can be examined in the Figure 8.1.
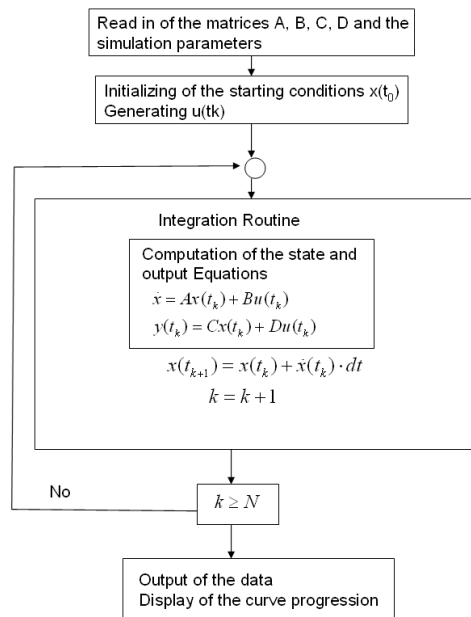

Figure 8.1: Flow Chart of the Matlab Simulation Program

8.2 Output Equation for the Simulation

The concept of the controllability is linked to the question whether if the input u affects or controls the variation of each one of the state variables x_i and if the system is then controllable. On the other hand if any of the state variables are not influenced by the input u, then the system is referred to as uncontrollable. As used in the Matlab simulation, the system is taken from a given initial state $x(0)$ to a specified final state $x(tf)$ using the available control u, then the system is controllable. The state equation of the used linear time invariant system for the Matlab simulation for the lateral and longitudinal motion is:

$$\dot{x} = Ax + Bu \tag{8.1}$$

The output equation for this system is defined as:

$$y = Cx \tag{8.2}$$

The feed forward matrix D is a zero matrix for the longitudinal and lateral motion as mentioned in Section 5.3, this is the reason for the new definition of the output equation as seen in Equation 8.2.

8.3 Motion related Matrices A, B and C of the AC 20.30

The matrix A for the longitudinal and lateral motions of the AC 20.30 is already defined in Sections 7.1.1 and 7.2.1 and therefore these matrices are here not introduced anymore. The appearance of matrix C is equal for the lateral and longitudinal motion, because the system state and system output are equal and therefore the output matrix is defined as identity matrix as seen in Equation 8.3:

$$C = \begin{pmatrix} 1 & 0 & 0 & 0 \\ 0 & 1 & 0 & 0 \\ 0 & 0 & 1 & 0 \\ 0 & 0 & 0 & 1 \end{pmatrix} \tag{8.3}$$

8.3.1 Driving Matrices B for the longitudinal Motion

As mentioned before the AC 20.30 is a non conventional aircraft configuration and therefore it could be possible that some discrepancies for the definition of the motion

related matrices appear. But the only difference in the flight dynamic definition between the conventional aircraft and the AC 20.30 in this thesis appears for the definition of the Driving matrix B, because the AC 20.30 has two separate located flap pairs, one pair is located at the rear end, while the other flap pair is located at the wing as for conventional aircraft usual. But in the flight dynamics there is no definition for this kind of problems known or introduced, where two flap pairs at different locations are separately deflected.

The Driving matrix B has to be modified in case of the additional control surface to simulate its influences to the aircraft motion as well. The method to introduce the additional flap pair to the motion simulation is to increase the number of columns of the matrix B and the dimension of the Control vector $\vec{u}$. The new definition of the Driving matrix B can be examined in the Equation 8.4:

$$B = \begin{pmatrix} X_{\delta_e} & X_{\delta_{F_{Wing}}} & X_{\delta_{F_{RearEnd}}} & -X_u & -X_w & 0 \\ Z_{\delta_e} & Z_{\delta_{F_{Wing}}} & Z_{\delta_{F_{RearEnd}}} & -Z_u & -Z_w & -U_0 \\ M_{\delta_E} & M_{\delta_{F_{Wing}}} & M_{\delta_{F_{RearEnd}}} & -M_u & -M_w & -M_q \\ 0 & 0 & 0 & 0 & 0 & -1 \end{pmatrix} \tag{8.4}$$

Thus, as seen in the Equation 8.4, the B matrix is one column greater than the definition of this matrix for a conventional aircraft. In order of the additional column of the B matrix the dimension of the control vector $\vec{u}$ for the longitudinal motion has to be adapted with one additional dimension. This dimension introduces the additional flap to the control vector, because otherwise the state equation is not solvable.

$$\vec{u} = \begin{pmatrix} \delta_e \\ \delta_{F\,(Wing)} \\ \delta_{F\,(RearEnd)} \\ u(g) \\ w(g) \\ q(g) \end{pmatrix} \tag{8.5}$$

Input Parameters for the Driving Matrices B of the longitudinal Motion

But before the elements of matrix B can be compiled, the derivatives of the significant coefficients and stability derivatives have to be defined. The derivatives of the coefficients are listed in the Table 8.1. So with these parameters the missing elements of the driving matrices B can be computed with the equations introduced in Section 5.4.2. The required control related stability derivatives for the driving matrices B for the longitudinal motion can be examined in Table 8.2, 8.3 and 8.4. The Table 8.2 shows the control related stability derivatives due to the elevator deflection, while the Table 8.3

Table 8.1: Derivatives of the Coefficients for the longitudinal Motion

$C_{l_{\delta_e}}$	0.3291 rad^{-1}
$C_{d_{\delta_e}}$	0.0043 rad^{-1}
$C_{m_{\delta_e}}$	-0.1071 rad^{-1}
$C_{l_{\delta_{f\,(RearEnd)}}}$	0.4573 rad^{-1}
$C_{d_{\delta_{f\,(RearEnd)}}}$	0.0264 rad^{-1}
$C_{m_{\delta_{f\,(RearEnd)}}}$	-0.0593 rad^{-1}
$C_{l_{\delta_{f\,(Wing)}}}$	0.2982 rad^{-1}
$C_{d_{\delta_{f\,(Wing)}}}$	0.0241 rad^{-1}
$C_{m_{\delta_{f\,(Wing)}}}$	-0.0448 rad^{-1}

shows the derivatives due to the deflection of the flap pairs located at the wing. The last Table shows the control related stability derivatives due to the deflection of the flap pair at the rear end. The other required stability derivatives are introduced in Table 7.2 of Section 7.1.1.

Table 8.2: Controll related Stability Derivatives due to the Elevator Deflection

X_{δ_e}	-0.1769 m $\cdot$ rad^{-1}s^{-2}
Z_{δ_e}	-13.4383 m $\cdot$ rad^{-1}s^{-2}
M_{δ_e}	-20.9719 rad^{-1}s^{-2}

Table 8.3: Controll related Stability Derivatives due to the Deflection of the Flaps located at the Wing

$X_{\delta_{F\,Wing}}$	-0.9938 m $\cdot$ rad^{-1}s^{-2}
$Z_{\delta_{F\,Wing}}$	-12.1762 m $\cdot$ rad^{-1}s^{-2}
$M_{\delta_{F\,Wing}}$	-6.6118 rad^{-1}s^{-2}

Table 8.4: Controll related Stability Derivatives due to the Deflection of the Flaps located at the Rear End

$X_{\delta_{F\,RearEnd}}$	-1.0798 m $\cdot$ rad^{-1}s^{-2}
$Z_{\delta_{F\,RearEnd}}$	-18.6711 m $\cdot$ rad^{-1}s^{-2}
$M_{\delta_{F\,RearEnd}}$	-11.6014 rad^{-1}s^{-2}

Appearance of the Driving Matrices B of the AC 20.30 for the longitudinal Motion

As mentioned before, there are two methods to define the Driving matrices of the longitudinal motion. The appearance of the B matrix can be examined in the Equation 8.6:

$$B = \begin{pmatrix} -0.1769 & -0.9938 & -1.0798 & 0.1037 & 0.8824 & 0 \\ -13.4383 & -12.1762 & -18.6711 & 0.6984 & 5.1478 & -20 \\ -20.9719 & -6.118 & -11.6014 & -0.2188 & 0.7572 & 2.85 \cdot 10^{-5} \\ 0 & 0 & 0 & 0 & 0 & -1 \end{pmatrix} \tag{8.6}$$

8.3.2 Motion related Matrices for the lateral Motion

Driving Matrix B for the lateral Motion

Before the Driving matrix B can be compiled, the aerodynamic aerodynamic coefficient derivatives caused by the aileron and rudder deflections have to be provided with the help of the wind tunnel test. These derivatives are listed in the Table 8.5. With the help of the derivatives introduced in Table 8.5 the control related stability derivatives for the lateral motion can be defined as shown in Table 8.6. Now with the values for the control related derivatives and the stability derivatives of Table 7.5 and Table 8.6 the Driving matrix B can be compiled as seen in Equation 8.7.

Table 8.5: Derivatives of the Coefficients for the lateral Motion

$C_{y_{\delta_A}}$	$0.0104 \ \mathrm{rad}^{-1}$
$C_{l_{\delta_A}}$	$-0.2334 \ \mathrm{rad}^{-1}$
$C_{n_{\delta_A}}$	$-0.0028 \ \mathrm{rad}^{-1}$
$C_{y_{\delta_R}}$	$0.0579 \ \mathrm{rad}^{-1}$
$C_{l_{\delta_R}}$	$0.0173 \ \mathrm{rad}^{-1}$
$C_{n\delta_R}$	$-0.0130 \ \mathrm{rad}^{-1}$

$$B = \begin{pmatrix} 0.4264 & 2.3639 & 0.5783 & 0 & 1.0 \\ -67.2281 & 4.9625 & 29.6669 & 5.0873 & -1.7042 \\ -0.8314 & -1.8519 & -4.7746 & 0.4157 & 0.1248 \\ 0 & 0 & 0 & -1 & 0 \end{pmatrix} \tag{8.7}$$

Table 8.6: Control related Stability Derivatives of the lateral Motion

Y_{δ_A}	$0.4264 \text{ rad}^{-1}\text{s}^{-1}$
L'_{δ_A}	$-67.2281 \text{ rad}^{-1}\text{s}^{-2}$
N'_{δ_A}	$-0.8314 \text{ rad}^{-1}\text{s}^{-2}$
Y_{δ_R}	$2.3639 \text{ rad}^{-1}\text{s}^{-2}$
L'_{δ_R}	$4.9625 \text{ rad}^{-1}\text{s}^{-2}$
N'_{δ_R}	$-1.8519 \text{ rad}^{-1}\text{s}^{-2}$

8.4 Short Introduction to the Main Functions of Matlab Simulink

8.4.1 Introduction to the Block Diagramm

A Matlab Simulink model is model of a dynamic system. It consists of a set of symbols referred to as blocks, which are interconnected with lines. Each block represents an elementary dynamic system, if it produces an output continuously then it is called continuous block or if it produces an output at specific points in time then it is called discrete block.

The lines used in Matlab Simulink represent connections of the block in- and outputs. The type of the used block describes the relationship between a block's output and it's output, states and time. A block consists of one of the following elements: a set of inputs, a set of state and a set of outputs. A block output is a function of time, blocks inputs and states if the blocks consists of all the three elements.

8.4.2 The Matlab Simulink Solver

A Matlab Simulink model specifies the time derivatives of its continuous states but not the values of the states. Hence, when Simulink is simulating dynamic systems, it must compute the continuous states with the help of numerical integration of its state derivatives.

There are plenty of numerical integration techniques, each having their advantages and disadvantages in their applications. The Simulink based solver is called ordinary differential equation (ODE) solver (for further information see **Zwillinger 2003**). For Simulink applications this solver is a good option, because it is the most stable, efficient and accurate method of these numerical integration methods. It can be specified to use in the model or when running a simulation.

8.5 Matlab Simulink Model for the Simulation

Now with all required inputs, e.g. defined matrices A, B, C and D, the simulation program for the lateral and longitudinal motion can be designed. It is based on the Matlab Simulink environment as mentioned before. For the firw longitudinal and lateral motion the same Matlab Simulink assembly is designed as seen in the Figures 8.2 and 8.3, because the structure of both programs is nearly equal, except the different matrix inputs and the additional control surface for the longitudinal motion. The complete structures of the simulations for the lateral and longitudinal motion can be seen at the following figures.
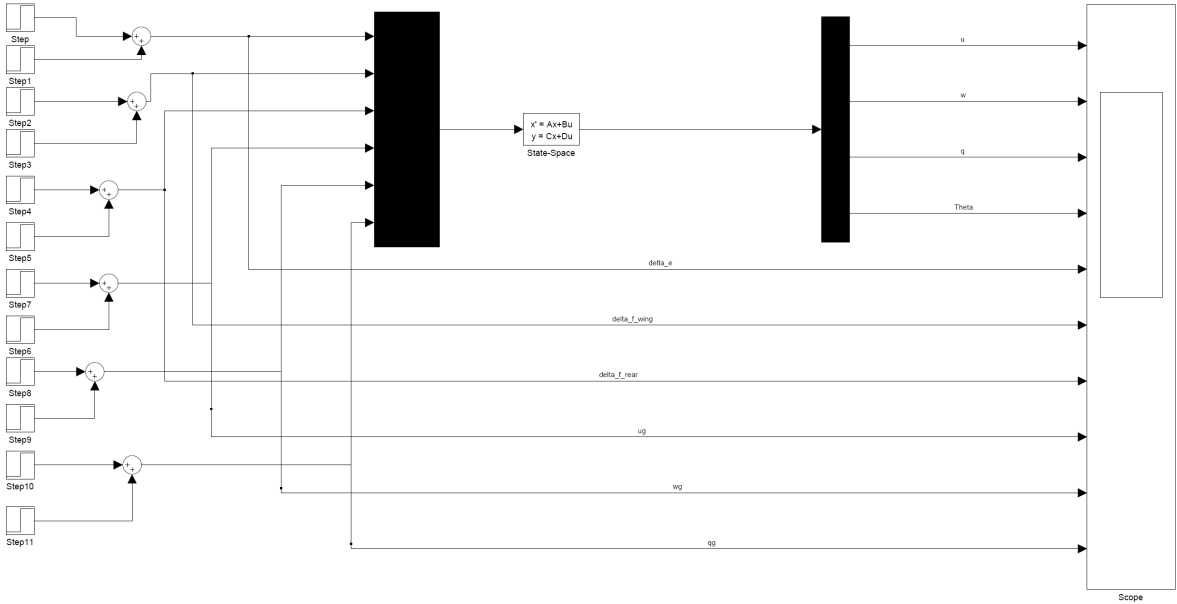
Figure 8.2: Structure of the Matlab Simulink Simulation of the longitudinal Motion
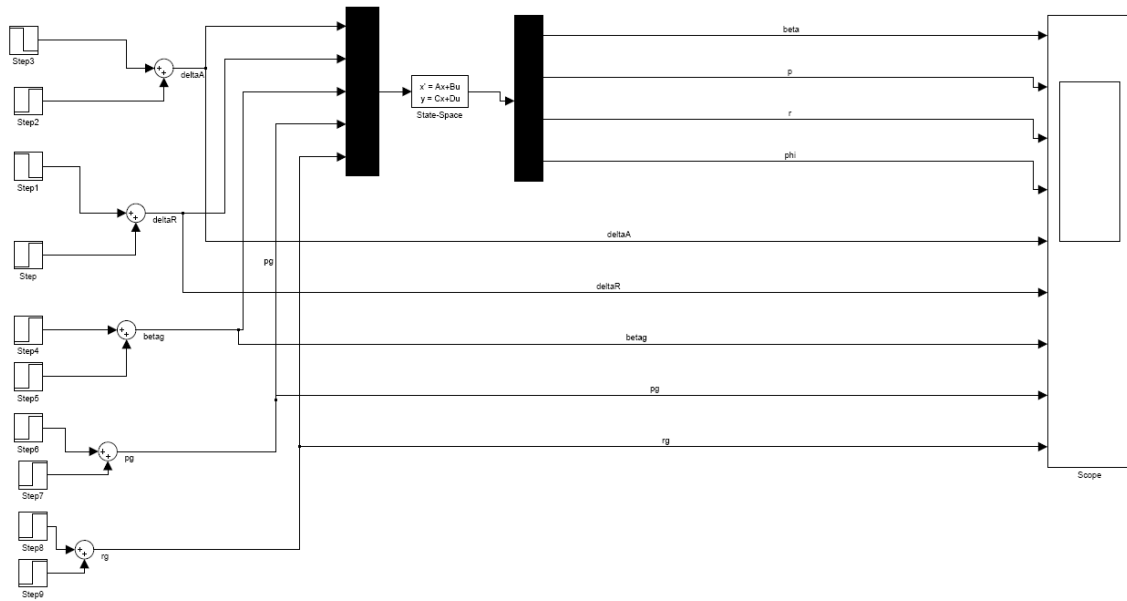
Figure 8.3: Structure of the Matlab Simulink Simulation of the lateral Motion

8.5.1 Introduction of the used Matlab Simulink Blocks

As seen in Fig. 8.2 the Matlab environment gives the opportunity to model control engineering problems with blocks. The used blocks of this program are introduced in this section.

The Block Step

The Step Block seen in Figure 8.4 provides a step between two definable levels at a specific time. If the step time parameter value is greater than the simulation time, the block's output is the initial parameter value. For simulation time greater or equal the step time, the output is the final value. The numeric parameters of the blocks must be of the same dimensions after the scalar expansion. The inputs for the block step for this simulation are the step time in seconds and the final value. The final value of the Step blocks, which belong to the control surfaces of an aircraft, is the angle of deflection in the unit rad, e.g. for a angle of 4° is has to be defined as $4 \cdot \pi/180$. The final value of the step blocks, which introduce the gust effects, has to be typed in the unit m/s to avoid dimension or unit problems. Two Step blocks belong to one introduces control surface or to one direction of a gust. The first blocks defines the time when the deflection or the gust starts, while the other step block defines the end of the deflection or of the gust.
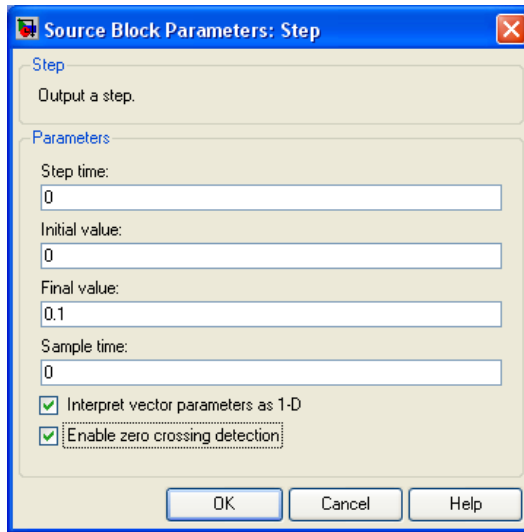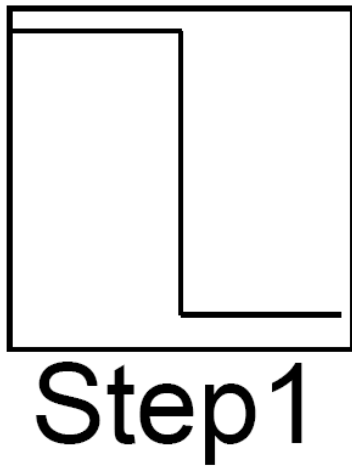
80

Figure 8.4: The Block Step Icon   **Figure 8.5:** Input Values for the Step Block

The sample time inputs have to be in the unit seconds for this simulation and it defines the time when the Step block value is influencing the simulated system, e.g. when the gust or the rudder deflection affects the aircraft. The Step blocks have marked the "Interpret vector parameters as 1-D", therefore the column or row matrix values for it's numeric parameters result in a vector output signal. The last option for the step block tool bar is also marked for the blocks the "Enable zero crossing detection", therefore the zero crossing detection to detect step times is enabled.
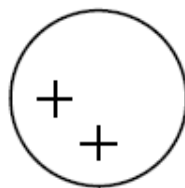
The Sum Block

Figure 8.6: The Sum Block Icon

The Sum Blocks executes addition or subtraction on its inputs. The elements for subtracting or adding can be scalars, vectors or matrices. It can also combine the elements of a signal. The Sum blocks have marked the "Interpret vector parameters as 1-D", therefore the column or row matrix values for the step block's numeric parameters result in a vector output signal. The last option for the step block tool bar is also marked

for both blocks the "Enable zero crossing detection", therefore the zero crossing detection to detect step times is enabled. The input of the parameter of the sumblock can be seen in the Figures 8.7 and 8.8, where the two input sheets are shown. For the first input sheet "Main" the input parameters can be examined in the Figure 8.7.

The first defined input parameter for this sheet is the Icon Shape field, which is defined as round. It designates the icon shape of the block. The input parameters for the "List of signs" for this simulation is $| + +$, that means that the input vectors are added, but with a space between the signs, which the input parameter $|$ defines. If one of them is required to subtracted, a minus $(-)$ has to be typed in. The input parameter for the sample time is -1, which defines the sample time as inherit. The "Signal Data Types" seen in Figure 8.8 is defined with the default settings. For further information see **Bode 2006**.
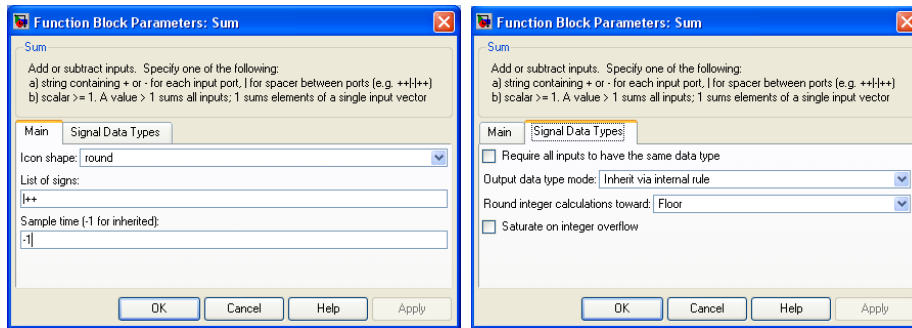

Figure 8.7: Input Parameters for the Sum Block

Figure 8.8: Input Parameters for Sum Block II

The State Space Block

The State Block examined in Figure 8.9 implements a system whose behaviour is explained by the state and output equations mentioned in Sections 5.2 and 5.3.

Figure 8.9: The State Space Block Icon

The block accepts one input and generates one output. The input vector width is determined by the number of columns in the B and D matrices. The output vector
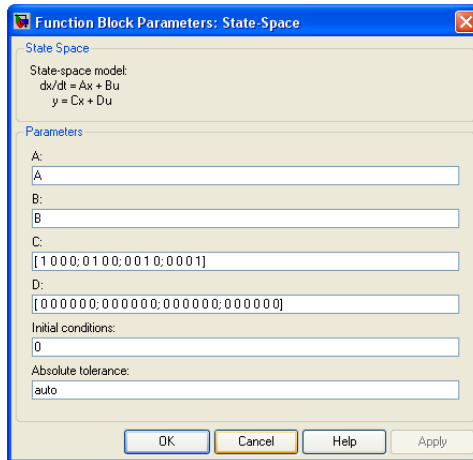
Figure 8.10: Input Parameter for the State Space Block

width is defined due to the number of rows in the C and D matrices. The Initial conditions can be set with a initial state vector if they have to be considered. The absolute tolerance is used to solve the block's states. The input parameter for it could be set with numeric value or with "Auto", if "Auto" is selected Simulink determines the determines the absolute tolerance. But if a numeric value is insert Simulink uses this value to scope the block's states.

The Demux Block

Figure 8.11: The Demux Block Icon

The block symbol of Figure 8.11 belongs to the Demux function. The Demux Block is a simply grouping operator, which extracts the components of an input signal and outputs the components as a separate signals. The output signals are ordered from top to bottom output ports. The number of output parameter allows to specify the number and optionally the dimensionality of each output port.
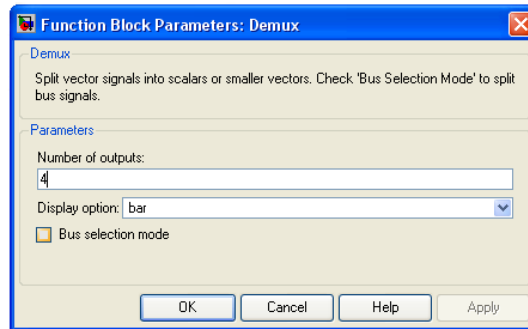
Figure 8.12: Input Parameters for the Demux Block

If no specification of the dimensionality of the outputs is required, the block determines the dimensionality of the outputs. For this simulation are four ports required as seen in Figure 8.12. Further the Bus Mode can be selected (further information about the Bus mode can be taken out of this the Matlab User guide **Matlab 2002**).
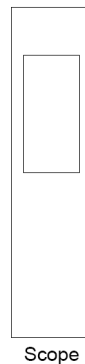
The Scope Block

Figure 8.13: The Scope Block Icon

The Scope Block, shown in Figure 8.13, displays its input with respect to simulation time. It could have multiple axes and all these axes have a common time range with independent y axis. The Scope Block allows to adjust the amount of time and the range of inputs values displayed. It just opens after a simulation, because then it can visualize its input signals. A output of the scope block can be visualized in the figure 8.14.
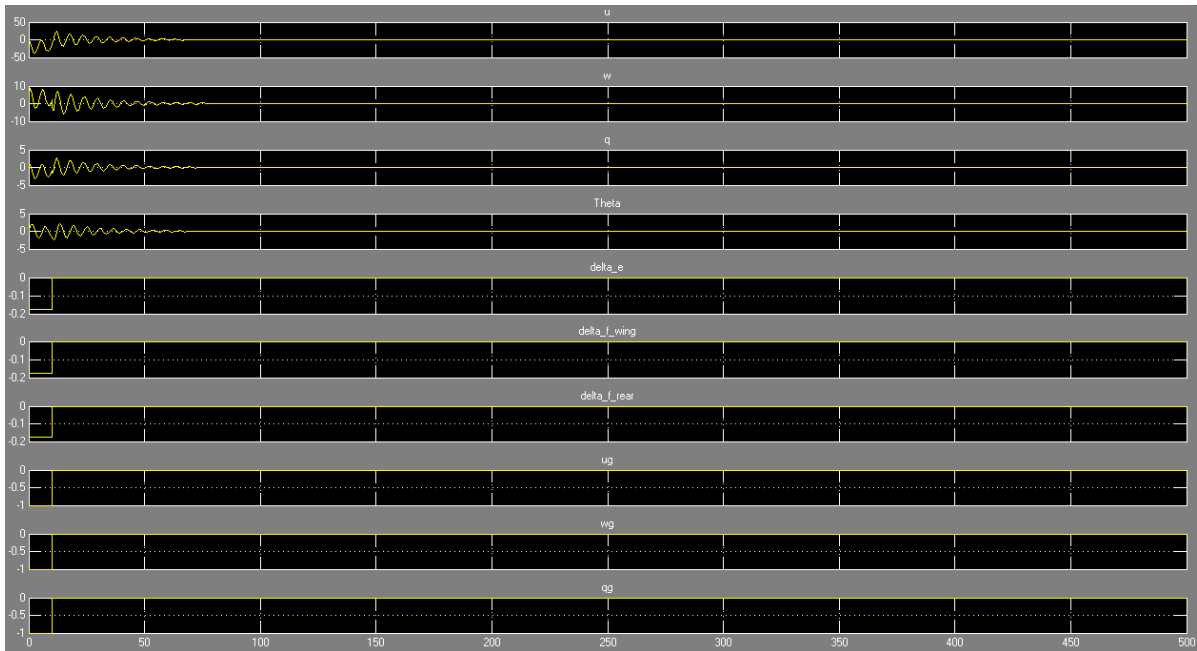
Figure 8.14: Output of the Scope Block Icon

Mux Block

The Mux Block symbol is shown in Figure 8.15. The Mux Block combines its input into a single output. Its input can be a scalar, vector or matrix signal. Depending on its input, the output of a Mux Block is a vector or a composite signal. If the input signals are vectors the output signal is a vector. If any input signal is not a vector, the output of the Mux block is a bus signal. The number of ports have to be set to four, as seen in Figure 8.16, to introduce the gust and the control surface deflections to the state equations.
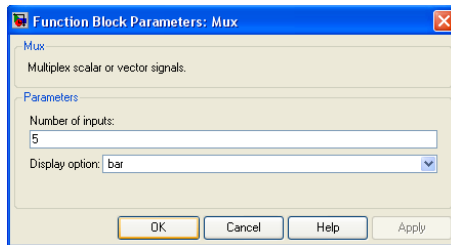

Figure 8.15: Simulink Symbol of the Mux Block

Figure 8.16: Input Data for the Mux Block

85

## 8.6 Interpretation of the Motion Simulation Results

This sections describes the graphical output of the Matlab Simulink simulation, where the main characteristic motion modes for the longitudinal and lateral motion are introduced and analyzed.

8.6.1 Motion Simulation Results for the longitudinal Motion

The motion simulation of the longitudinal motion simulates the flight behaviour of the AC 20.30 during flight maneuvers (controll surface deflections), gust appearance, and the flight behaviour during a Short Period mode and Phugoid mode.

Flight Behaviour during Control Surface Deflections and Gust Appearance

After the run button of Simulink is pressed, it computes the aircraft motions for a previous defined time interval, control surface deflection and/or gust appearance. The first four scope columns of Figure 8.17 belong to the previously defined motion directions of the aircraft. So as seen in this Figure, the aircraft damps out the disturbance of the system introduced through the control inputs or a gust appearance by itself as expected for a statically and dynamically stable aircraft. The columns "deltae" and "deltaf" of Figure 8.17 shows the deflection, when the deflection starts (x-axis) in seconds and the value of the deflection (y-axis) in the unit rad. The last three columns of the scope output window "ug", "wg" and "qg" of the Figure belong to the gust introduction for the simulation. They show the directions of a potential gust, if values are typed in for this directions in the relevant Step Blocks. The x-axis of each column belong to the moment the gust should appear in the simulation in seconds and the y-value belong to the size of the gust and its unit is in m/s as mentioned before.
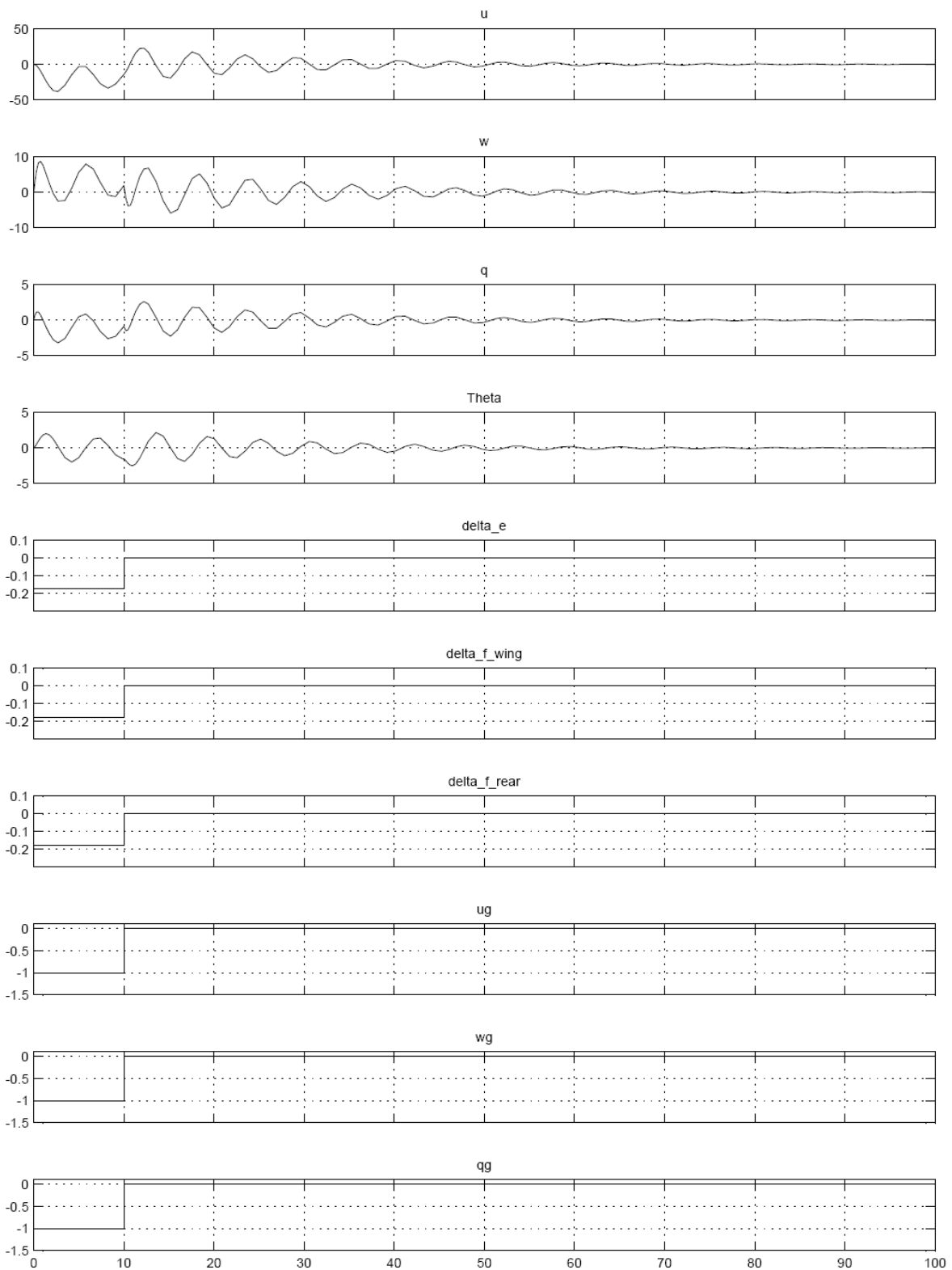
Figure 8.17: Output of the Flight Behaviour for the longitudinal Motion during Disturbances

87

Flight Behaviour in the Short Period Mode

The flight characteristics of the AC 20.30 in the Short Period mode can be simulated by setting the initial value of the w-direction in the state equation menu $\neq 0$, while no gust appear or control surfaces are deflected. Then the aircraft is adjudged in the Short Period Mode with this initial conditions. The behaviour in this mode can be examined in the Figure 8.18, where the aircraft behaviour in the four directions is plotted. So with the help of this figure the frequency of the Short Period mode can be graphically determined and can be checked wit the computed values of Section 7.1.3. With the measured wavelength T the frequency of the Short Period mode ω_{sp} can be determined with following equation:

$$\omega_{sp} = \frac{2\pi}{T} \tag{8.8}$$

With $T \approx 4$s leads to a frequency $\omega_{sp} = 1,5708 \text{ rad} \cdot \text{s}^{-1}$. The difference in the frequency between the measured and the computed values appears, because the Phugoid and the Short Period modes superimpose each other. To avoid this superpositions of these modes a feedback system should be introduce to the system.
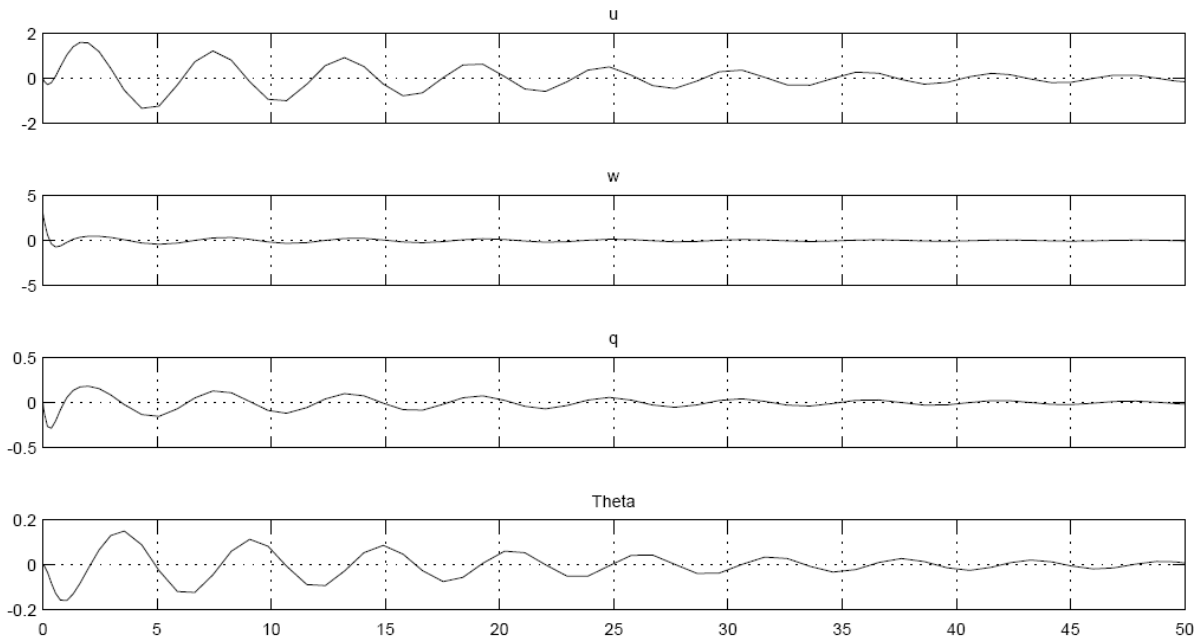

Figure 8.18: Output of the Flight Behaviour in the Short Periode

The AC 20.30 is able as, seen in Figure 8.18, to damp the animation introduced in the system for the Short Period mode. This has to deal with the fact, that the computed values of the damping ratio for the Short Period mode and for the Phugoid mode are

positive. The damping ratio of the Phugoid mode is also important for mode, because, as mentioned before, in this simulation it is not possible to avoid the superposition of these modes.

Flight Behaviour in the Phugoid Mode

The behaviour of the AC 20.30 in the Phugoid mode can be shown, if in the initial conditions menu the θ-value has to be set $\neq 0$. As for the Short Period mentioned the frequency of the Phugoid mode can be determined with Equation 8.8 and the measured wavelength of this mode. It can be measured in Figure 8.19, where the four directions of the AC 20.30 caught in the Phugoid mode are plotted. The measured value of T is for the Phugoid mode $T = 6$ s, which leads to a frequency of $\omega_{ph} = 1.0472$ rad $\cdot$ s^{-1}. But different as for the Short Period mode the computed frequency and the graphically determined frequency a nearly equal. The small difference of this two values can be traced back to the error in reading of the motion plots. In case of the small chosen number of time steps, the damping ratio of the Phugoid mode is hardly to see.
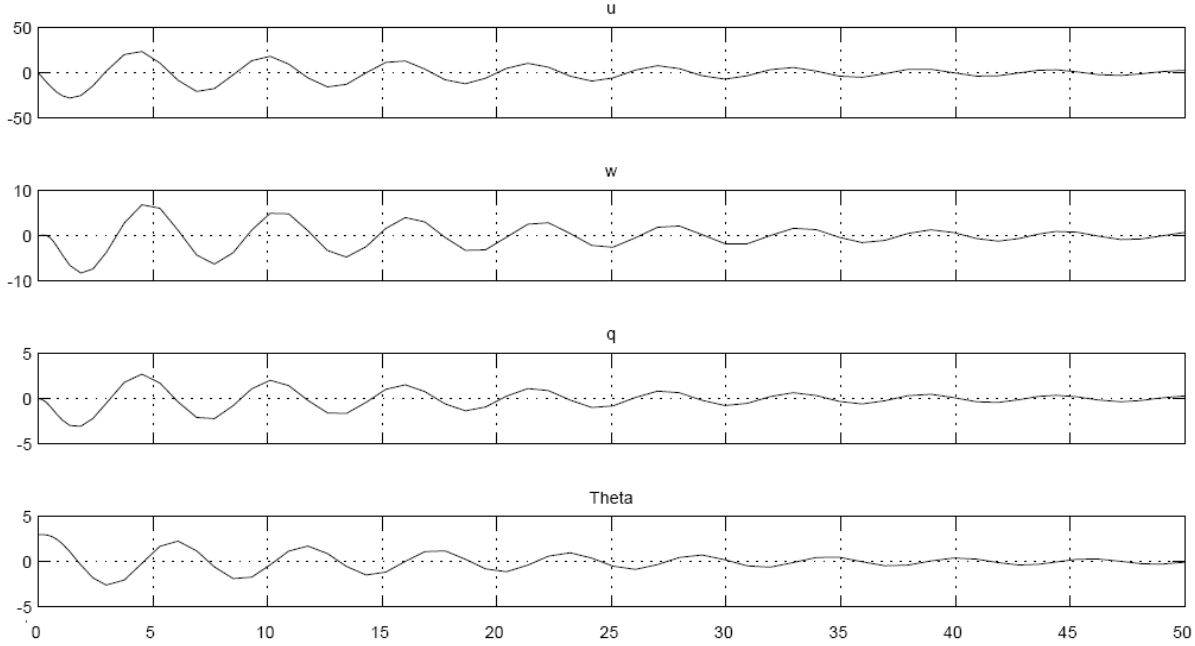

Figure 8.19: Output of the Flight Behaviour in the Phygoid Mode

The AC 20.30 behaves during the Phugoid mode simulation as expected. It damps out the disturbances caused to the Phugoid mode.

8.6.2 Motion Simulation Results for the lateral Motion

This subsection describes the flight behaviour of the AC 20.30, during suddenly appearing gusts in the lateral motion and control surface inputs in the lateral motion, besides this the flight behaviour of the AC 20.30 is investigated in the three main modes (Dutch Roll, Roll and Spiral Mode) for the lateral motion.

Flight Behaviour during Control Surface Deflections and Gust Appearance

The scope output of Matlab Simulink for the lateral motion with the help of the previous defined control vector for the lateral motion can be examined in Figure 8.20. Different as expected the AC 20.30 is not able to damp the disturbances of the lateral motion, which appear after the aircraft experiences control inputs or gusts in the lateral motion. This behaviour of the AC 20.30 can be good examined in the first four outputs ports (Figure 8.20) of the Scope block.

Instead of decreasing the amplitude of the four motion curves with a rising number of time steps, the aircraft characteristics of the AC 20.30 for the lateral motion increase the amplitude and frequency of these curves. As seen in the columns of the scope block, which show the time and value of the introduced control surface deflection and/or gust appearance, a small deflection of e.g. the aileron is enough to bring the aircraft in an unstable flight phase.

So the AC 20.30 shows a dynamically unstable behaviour for the lateral motion. For dynamically stable flight chracteristics the AC 20.30 requires additional dampers in the lateral motion to avoid unstable flight characteristics. The reason for this flight characteristic could be the computed dynamic instability of the Spiral Mode.
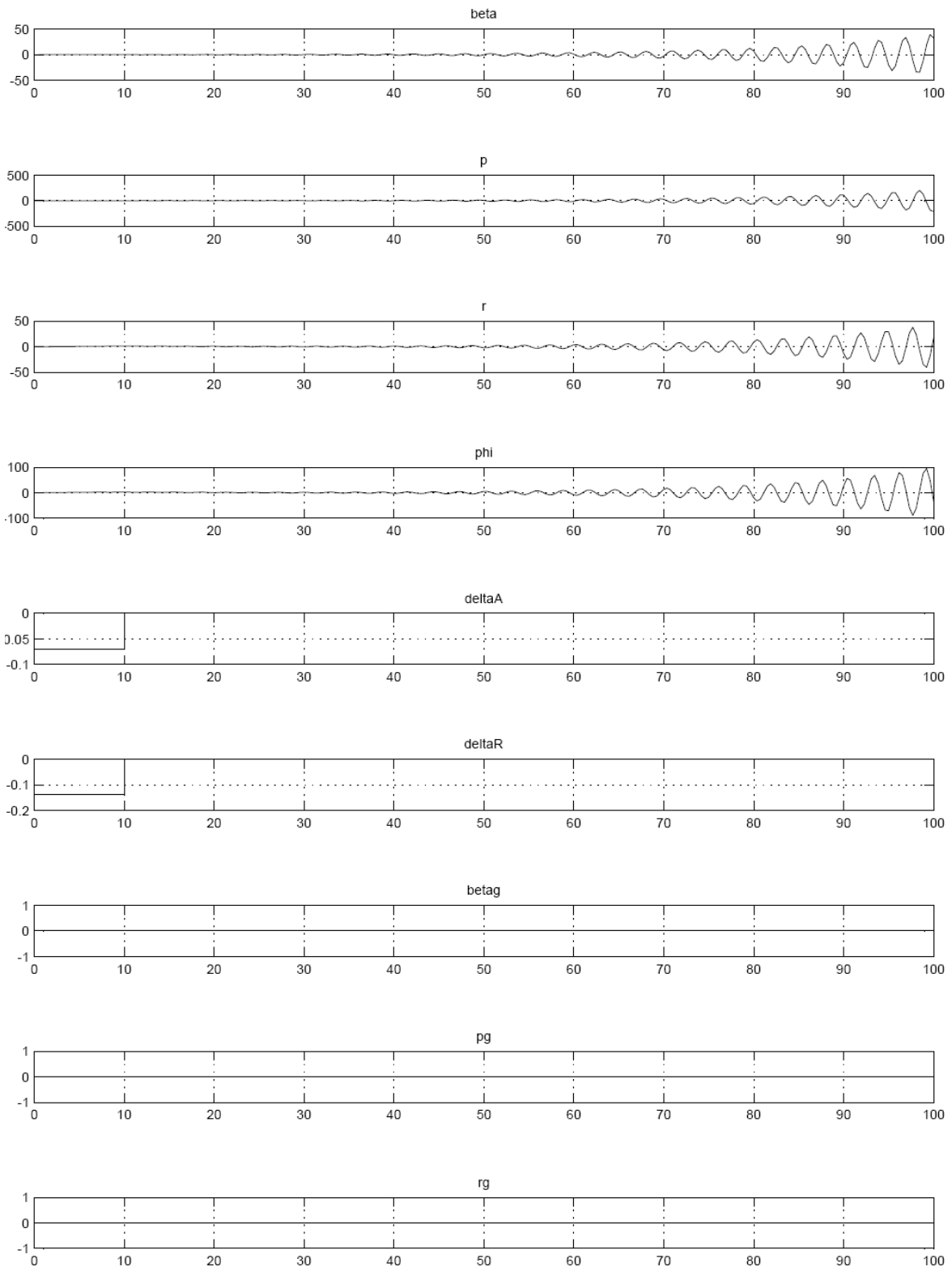
Figure 8.20: Output of the Flight Behaviour for the lateral Motion during Disturbances

91

Flight Behaviour in the Dutch Roll Mode

The Dutch Roll mode can be simulated in the Simulink envioronment, if in the initial condition menu of the state equation block the β-value is set to $\beta \neq 0$. The aircraft behaviour in the Dutch Roll mode can be examined in Figure 8.21, where the four flight directions of the AC 20.30 for the lateral motion are plotted.
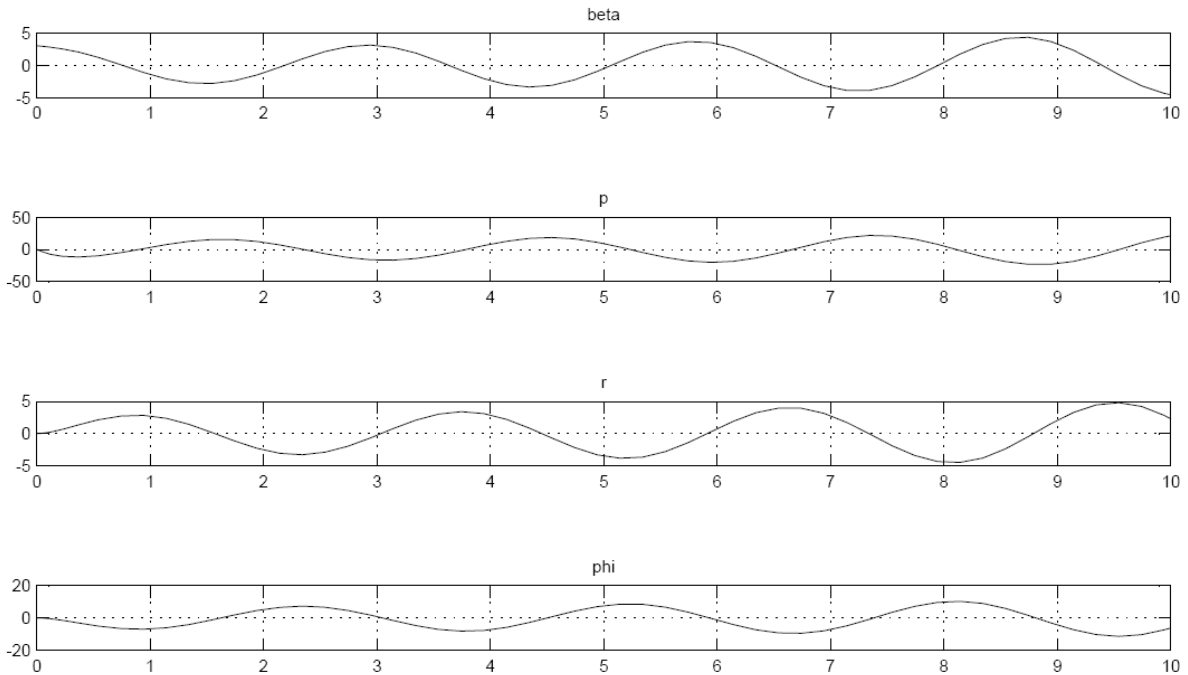

Figure 8.21: Output of the Flight Behaviour for the lateral Motion during Disturbances

With the help of these plots the wavelength can be graphically determined and therefore the frequency ω_D for the Dutch Roll mode can be computed with the help of the Equation 8.8 introduced in Section 8.6.1. The wavelength for the Dutch Roll mode is $T_D \approx 3$ s. The frequency ω_D determined with this method has following value: $\omega_D = 2.0944 \text{ rad} \cdot \text{s}^{-1}$. This value is really close to the computed value introduced in Section 7.2.3 ($\omega_D = 2.2015 \text{ rad} \cdot \text{s}^{-1}$). The small difference in the values of the frequency belongs to the error in reading for the wavelength.

There is no damping behaviour visible for the Dutch Roll mode in the shown time interval of Figure 8.21. The fact for this behaviour is the small computed damping ratio of the AC 20.30 for the Dutch Roll mode in Section 7.2.3 ($\xi_D = 0.1597$).

9 Future Prospective

9.1 Required Coefficients for upcoming Investigations

For upcoming investigations the aerodynamic derivatives C_{l_r}, C_{l_p}, C_{n_r} and C_{l_p} have to be measured for the AC 20.30, because for this thesis the values are taken out of a PhD thesis, where a similar Blended Wing Body configuration was investigated. Another parameter, which has to be measured, is the $C_{m_{\dot{\alpha}}}$ derivatives to compute the "Tilde" derivatives.

9.2 Damper for the lateral Motion

As seen in the Figures of the previous chapter the AC 20.30 shows for the lateral motion are dynamically unstable behaviour. To damp these motions and avoid this unstable behaviour during disturbances, the AC 20.30 requires additional damping elements. But under the given time was it not possible to deal with the additional damping elements. For the existing Simulink simulation the autopilot could be introduced to provide lateral stability. The autopilot deflects the control surfaces automatically without human being assistance.

10 Conclusion

This thesis is about a flight dynamic stability investigation and motion simulation of the Blended Wing Body aircraft configuration for the longitudinal and lateral motion.

The stability investigation is based on the aerodynamic coefficients and derivatives measured at the wind tunnel Dresden. With the help of these coefficients and derivatives it is possible to determine the required stability derivatives for the longitudinal and lateral motion. The static stability is given for the AC 20.30 for the longitudinal and lateral motion, because the stability, which defines the flight characteristics of an aircraft for the static stability, accomplish all required constraints for a static stable flight behaviour of the AC 20.30. Before the dynamic stability of the AC 20.30 can be investigated, the coefficient matrices A have to be determined for the longitudinal and lateral motion with the help of the stability derivatives.

For the longitudinal motion the AC 20.30 is dynamically stable behaviour, because all eigenvalues of the coefficient matrix A for the longitudinal motion have negative values for the real parts. With the computed eigenvalues the flight qualities of the AC 20.30 can be determined for the Phugoid and Short Period mode, because the determination of the flight quality for the modes is a function of the damping ratio, which can be computed again with the help of the eigenvalues. The Control Anticipation Parameter is different as the two other modes a function of the naturally frequency of the Short Period mode and the acceleration sensitivity. For all three here introduced modes a flight level 1 characteristics for a category B flight phase situation, therefore the AC 20.30 is a flight level 1 aircraft for the longitudinal motion.

The eigenvalues of the coefficient matrix for the lateral motion are negative or have negative real parts of their value, besides one eigenvalue, which belongs to the Spiral mode, has a positive real eigenvalue. Therefore the AC 20.30 is dynamically unstable for the Spiral mode, but dynamically stable for the Dutch Roll and Roll mode. Now with the computed eigenvalues the flight qualities for the lateral motion of the AC 20.30 can be classified for the relevant motion modes. The flight quality of the Dutch Roll mode is a function of its damping ratio and its naturally frequency. With the computed values of the damping ratio and frequency the AC 20.30 shows flight quality level 1 characteristics for the Dutch Roll mode. Different as for the Dutch Roll mode the flight quality of the Spiral and Roll modes are functions of time parameters (Time to Double for the Spiral mode and Damping Time for the Roll mode). With the computed values of these time parameters the AC 20.30 is classified in Level 1 for the flight qualities of the Roll mode

and in level 2 for the flight qualities of the Spiral Mode. This results in the level 1-2 for the overall flight characteristics of the lateral motion.

The last part of this thesis deals with the motion simulation of the AC 20.30 for the longitudinal and lateral motion. The motion simulation is designed in the Matlab Simulink environment. It requires the matrices for the state equation additional to the coefficient matrix. These matrices are the Driving matrix, Output matrix and the Feed Forward matrix. The motion simulation shows the aircraft flight behaviour, if the aircraft is affected by control inputs or gust disturbances. For the longitudinal motion the AC 20.30 is able to damp all disturbances, so that the aircraft is in stable conditions afterward. Different the situation for the lateral motion, where the AC 20.30 is not able to damp the disturbance, and the aircraft is after a disturbance in unstable flight conditions. As a result of this the AC 20.30 requires additional damper for the lateral motion.

11 Final Remark

The subject of the thesis *Flight Dynamic Investigation of a Blended Wing Body Aircraft* deserves in the beginning an acquainting into a complex subject area. This thesis describes the flight characteristics of a Blended Wing Body flight model. This investigations are a first step to describe the flight characteristic of a real size Blended Wing Body Aircraft, which have to be investigated in an upcoming thesis. But I think this thesis gives a good insight view of the main flight dynamic characteristics of the AC 20.30.

Through the attending of this thesis and the involved researches, one obtain a good overview of the coherences in flight dynamics for the flight characteristics of an aircraft. I hope, that this thesis gives a good overview of the flight dynamic characteristics of the AC 20.30 and that it can perhaps provide a basis for upcoming investigations of this aircraft.

References

AIRLINES 2006   Airliners: URL: http://.www.airliners.net

Anderson 2001   ANDERSON, John, D. Jr: *Aircraft Performance and Design*, WCB/Mc Graw-Hill, New York/San Francisco, 2001

Bode 2006   BODE, Helmut: *Matlab Simulink – Analyse und Simulation dynamischer Systeme*, Teubner, Wiesbaden, 2006

Castro 2003   CASTRO, Helena, V.: *Flying Qualities of a Fly by Wire Blended Wing Body Civil Transport Aircraft*, Phd Thesis, Technical University Delft, Delft, 2003

Clean 2003   MC CLEAN, Donald: *Automatic Flight Control Systems*, Prentice Hall, New York, 1990

Danke 2005   DANKE, Kevin: *Flugerprobung mit einem BWB-Flugmodell*, Dipl-oma Thesis, University for applied Science Hamburg, Hamburg, 2005 URL: http:\\bibiliothek.ProfScholz.de

Brockhaus 2002   BROCKHAUS, Rudolf: *Flugregelung*, Springer Verlag, Berlin /Heidelberg/New York, 2001

Matlab 2002   MATHWORKS: *Simulink-Model Based and System Based Design*, The Mathworks Inc., Natick, 2002

Nelson 1998   NELSON, Robert, C.: *Flight Stability and Automatic Control*, WCB /McGraw-Hill, New York/San Francisco, 1998

Pamadi 1998   PAMADI, Bandu, N.: *Performance, Stability, Dynamics and Control of Airplanes,* AIAA Education Series, Virgina, 1998

Raymer 1995   RAYMER, Daniel, P.: *Aircraft Design: A Conceptual Approach,* AIAA Education Series, Washington D. C., 1995

Reichert 1987   REICHERT, G: *Lectures Notes Flugmechanik III, Flugeigenschaftskriterien / Aktive Steuerung*, Institut für Flugmechanik, Technical University Braunschweig, 1987

Schlichting I   SCHLICHTING Herman, TRUCKENBRODT, Erich: *Aerodynamik des Flugzeuges Band I*, Springer Verlag, Berlin/Heidelberg/New York, 1967

Schlichting II   SCHLICHTING Herman, TRUCKENBRODT, Erich: *Aerodynamik des Flugzeuges Band II*, Springer Verlag, Berlin/Heidelberg/New York, 1967

Scholz 1999   SCHOLZ, Dieter: *Skript zur Vorlesung Flugzeugentwurf*, University for applied Science Hamburg, Hamburg, 1999

Scholz 2007   SCHOLZ, Dieter: *Skript zur Vorlesung Flugmechanik II*, University for applied Science Hamburg, Hamburg, 2007

Schulze 2007   SCHULZE, Detlef: *Aerodynamik mit Labor Vorlesungsskript*, University for applied Science Hamburg, Hamburg, 2007

Zingel 2006   ZINGEL, Till: *Auswertung Windkanalversuche am BWB-Modell AC 20.30*, University for applied Science Hamburg, Hamburg, 2006

Zingel 2007   ZINGEL, Hartmut: *Skript zur Vorlesung Flugmechanik*, University for applied Science Hamburg, Hamburg, 2007

Zwillinger 2003   ZWILLINGER, Daniel: Handbook of Differential Equations, Academic Press, Boston, 1997